RACE for 2030
RELIABLE
AFFORDABLE
CLEAN
ENERGY

B1 Research Project

Electrifying the Cold Chain - Phase 1: Concept Development

Final Report

Project team

University of South Australia

- Frank Bruno
- Ming Liu
- Soheila Riahi
- Michael Evans
- Peter Pudney
- Lachlan Mudge

DEM (SA)

- Joanne Galley
- Peter Nattrass

Aldom

- Mark Haig
- Jurij Polischko
- Darren Harris

Simble

- Bill McGhie

Project partners

Acknowledgements

Acknowledgement of Country

The authors of this report would like to respectfully acknowledge the Traditional Owners of the ancestral lands throughout Australia and their connection to land, sea and community. We recognise their continuing connection to the land, waters and culture and pay our respects to them, their cultures and to their Elders past, present, and emerging.

What is RACE for 2030?

RACE for 2030 CRC is a 10-year cooperative research centre with AUD350 million of resources to fund research towards a reliable, affordable, and clean energy future. https://www.racefor2030.com.au

Disclaimer

Executive Summary

The cold chain is a low temperature-controlled supply chain to prolong shelf life and maintain the quality of perishable products. Worldwide, the cold chain is reported to account for 30% of total energy consumption. The low temperature is achieved by using refrigeration facilities, such as cold storage rooms, refrigerated display and storage cabinets and refrigerated transport. Of particular concern is food transport refrigeration, which is responsible for 15% of world fossil fuel energy. Diesel engine driven vapour compression is dominant in transport refrigeration systems. This type of engine is noisy and has low efficiency of 35%-40% and very high CO_2-e emissions. In addition, the poor temperature performance of existing systems on diesel trucks is a key contributor to food spoilage.

This project has reviewed three commercial transport refrigeration systems, vapour compression, cryogenic and eutectic refrigeration. A concept design has been developed for an innovative eutectic refrigeration system suitable for use in both diesel and electric, light to medium refrigerated vehicles.

The on-board eutectic refrigeration system is the integration of an electric-powered refrigeration unit and a phase change thermal energy storage unit. The storage unit is electrically charged when the vehicle is not in service. This reduces the fuel consumption for diesel driven vehicles, or the load placed on the battery system for electric vehicles. Different from existing distributed eutectic systems, the proposed centralised design has the advantages of easy maintenance and better temperature control.

The novel system improves the energy productivity of cold chain logistics by reducing diesel fuel consumption and improving temperature control with more efficient refrigeration. For a medium size vehicle, a 70% reduction of CO_2-e emissions could be achieved for the refrigeration system if charging is provided by grid electricity in South Australia. The techno-economic analysis concluded that, compared to diesel-powered and battery-powered vapour compression refrigeration, eutectic refrigeration has the lowest energy consumption and operating cost.

Future work aims to construct a prototype eutectic refrigeration system and demonstrate its operation on a medium sized vehicle in South Australia.

Table of Contents

List of Figures

List of Tables

1. Introduction

With an increasing population, Australia's food demand and food production have continuously grown in recent decades. Retail sales of food costs over $140 billion per year in Australia (Department of Agriculture, 2014). Refrigeration is required through the entire supply chain to maintain the quality and freshness of perishable foods, such as vegetables, fruits, meats, seafoods and dairy products. In 2018, more than 23 million tonnes of foodstuffs worth $42 billion (based on farm gate values) passed through the Australian food cold chain (Brodribb & McCann, 2020). Worldwide, the cold chain is reported to account for 30% of total energy consumption (Adekomaya et al., 2016). In addition, according to the Australian Food and Grocery Council, food is moved in and out of refrigeration control very frequently, on average 14 times before consumption (Australian Food and Grocery Council, 2017). In one Australian study, before reaching consumers, broccoli took 39 steps along the cold chain (Han, 2005).

Refrigerated transport plays a crucial role in cold chain logistics. It is estimated to account for 60% of the total cost in cold chain logistics (Food Logistics, 2008). The transport refrigeration system is dominated by diesel-driven mechanical vapour compression with refrigerant R404A, which is the main refrigerant used in low temperature applications. Due to the large variation in operating conditions, the mobile refrigeration system has a very low coefficient of performance (COP: 0.5 ~ 1.75), resulting in high diesel consumption and CO_2-e emissions (Tassou et al., 2009). In Australia, refrigeration systems on trucks consume 70-90 million litres of diesel annually (Mark Ellis & Associates Pty Ltd, 2009), which generates 190-245 kilotonnes of CO_2-e emissions (national greenhouse accounts factor of 2.717 kg CO_2-e per litre of diesel (Department of Climate Change, 2022)) and costs about AUD$140-180 million (AUD$2 per litre of diesel). It has been reported that the worldwide refrigerated transport sector consumes around 15% of fossil fuel energy (Adekomaya et al., 2016).

R134A, R404A, R417B are commonly used refrigerants in refrigerated transport, which have a major impact on global warming. They have high global warming potential (GWP) of 1,430, 3,922 and 3,027, respectively, and are being phased out in developed countries (SOLGroup, 2022). Out of these refrigerants, R404A dominates refrigeration systems used in frozen food applications. Due to vibrations during transportation, on-board refrigeration systems have an additional risk of refrigerant leakage compared to stationary refrigeration systems. When leaks occur, the energy efficiency of the system is also reduced and the refrigerant needs to be refilled regularly.

The refrigerated transport sector is facing increasing pressure to adopt new technologies to decarbonise. This can be achieved through improving the energy efficiency of the refrigeration system, electrifying the refrigeration system using electricity from renewable energy sources, adopting alternative refrigeration technologies, and using alternative fuels from renewable energy sources. The promising renewable energy sources include liquid biofuels (ethanol and biodiesel), biogas (converted to CNC and LNG) and green hydrogen to power either conventional or adapted internal combustion engines (A2EP (Australian Alliance for Energy Productivity), 2017c).

Chapter 2 of this report presents the various types of transport refrigeration systems and technologies that can help to improve their performance. Chapter 3 reviews phase change materials that have potential to maintain the refrigerated space at frozen temperature (-18°C) and summarises test results of candidates selected for further study. Chapter 4 presents the methodology used for a techno-economic analysis of the various types of systems along with results, while Chapter 5 provides a concept design for a vehicle using eutectic refrigeration and then models the performance. Finally, Chapter 6 discusses different schedules of charging patterns and Chapter 7 provides conclusions to the study.

2. Transport Refrigeration Systems

2.1 State-of-the-art technologies

2.1.1 Vapour compression refrigeration

The vapour compression refrigeration (VCR) cycle dominates refrigeration systems used in refrigerated transport. This consists of mainly four components: evaporator, compressor, condenser and expansion device. There are mainly four types of compressor drive methods: auxiliary diesel unit, direct belt drive, auxiliary alternator unit and vehicle alternator unit (Maiorino et al., 2021). Most medium to large refrigerated vehicles have employed auxiliary diesel engine driven systems, a schematic diagram of which is presented in Figure 1. The other three options are commonly found in small trucks and vans.
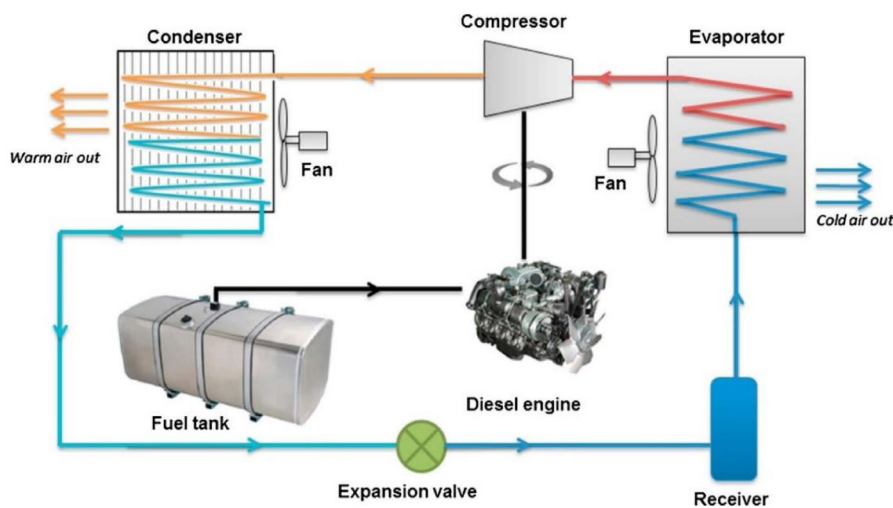
Figure 1. Schematic diagram of vapour compression transport refrigeration unit driven by a diesel engine (*Rai & Tassou, 2017*).

In 2009, the existing stock of truck refrigeration units in Australia was 21,150 (Mark Ellis & Associates Pty Ltd, 2009) and this number grew rapidly to 45,100 in 2018 (Brodribb & McCann, 2020). A comparison of the number of refrigerated vehicles in different categories are presented in Table 1. These truck refrigeration systems are estimated to consume 70-90 million litres of diesel per year, accounting for 5% of the total diesel consumption in Australia (Mark Ellis & Associates Pty Ltd, 2009).

Table 1. Stock of truck refrigeration units in 2009 and 2018 (*Brodribb & McCann, 2020; Brodribb et al., 2021; Mark Ellis & Associates Pty Ltd, 2009*).

Market Description	Technology	Application	Ave. refrigeration capacity rated at 2°C	Existing stock			
				2009	2012	2016	2018
Trailer & Inter-Modal	Transport refrigeration units	Articulated trailers up to 48 ft	18 kW	4,300	6,300	9,900	12,000
Diesel Drive		Rigid market 3-8 ton trucks (6-18 pallet)	4 – 10 kW	3,500	5,000	7,200	8,400
Off Engine	Vehicle powered (optional electrical stand-by)	1-4 ton trucks	1 – 5 kW	13,350	17,600	20,800	24,700
Total				21,150	28,900	37,900	45,100

2.1.2 Cryogenic refrigeration

Cryogenic refrigeration uses liquid nitrogen (LN_2, 3 bar) or liquid carbon dioxide (LCO_2, 8.6 bar) to maintain the space at the desired temperature. Commercial products are available on the market. There are three types of cryogenic systems: (1) direct injection of cryogenic fluid into the refrigerated space; (2) expanding cryogenic fluid in a heat exchanger and dispersing it into the atmosphere and (3) hybrid cryogenic refrigeration with a VCR system to allow for a quick pull down. Compared to VCR systems, cryogenic systems have the benefit of rapid pull-down of temperature, very low noise during operation, low energy consumption and reduced environmental impact. However, due to the relatively high cost of the cryogenic fluid, the market penetration of cryogenic refrigeration only accounts for 1% (Swahn, 2008) (based on statistics from 2008). In Europe, 0.5% of the sold truck and trailer refrigeration units are cryogenic refrigeration based on a personal communication with Thermo King in 2014, reported in Air Resources Board, 2015.

Figure 2 illustrates a liquid CO_2 ST-CR 300 transport refrigeration system developed by a major refrigerated transport supplier – Thermo King. Even though the CO_2-e emissions using the LN_2 and LCO_2 system is low compared to that of the VCR system during operation, the total emissions are equal in both systems if the emissions for producing diesel fuel, refrigerant and cryogenic fluid are considered.
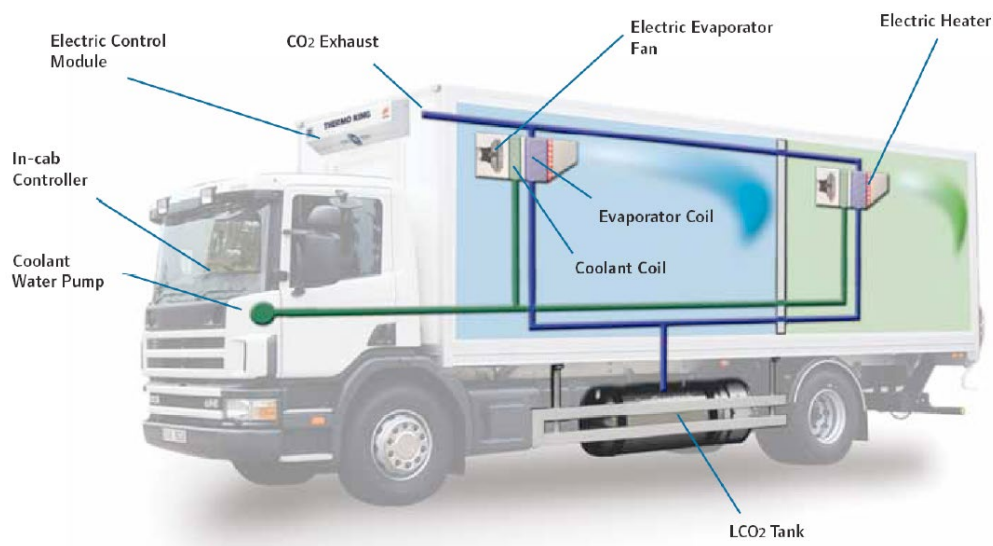
Figure 2. Thermo King liquid CO2 ST-CR 300 transport refrigeration system (Tassou et al., 2009).

Another type of commercially available cryogenic system uses liquefied natural gas (LNG) for both refrigeration and as the fuel source for the vehicle. LNG is contained in a tank at a temperature between -140°C and -120°C and a pressure ranging from 5 to 8 bar. Prior to use, LNG transitions from liquid to gaseous state, absorbing about 900 kJ/kg of energy, which can be used for air conditioning or refrigeration in vehicles (Maiorino et al., 2021).

2.1.3 Eutectic refrigeration

Latent heat thermal energy storage employing phase change materials (PCMs), commonly known as eutectic refrigeration, has been used in combination with a VCR system. The eutectic solution can store and release thermal energy at a defined temperature, which minimises the temperature fluctuation and offers better temperature management. Both the eutectic refrigeration and VCR systems are on the

vehicle. The eutectic solution is usually contained in flat, thin plates, which are located under the roof and on the front (as shown in Figure 3) to minimise the space requirements. The type of eutectic solution and the number of plates is determined by the desired temperature of the space and the refrigeration load, respectively. This system is charged using an electric refrigeration unit when the vehicle is not in service. During charging, the eutectic solution is frozen to store the energy. The stored cold energy is withdrawn by natural convection and radiation during transportation when cooling is needed.

There are a number of companies that supply the eutectic refrigerated bodies, for example, Eutectic (www.eutecticcar.com), Thermaxx (thermaxx.com.au), Carlsen Baltic (www.carlsenbaltic.com), Therma Truck (www.therma-truck.com.au) and Framec Truck (www.framectruck.com).

Eutectic refrigeration has the following advantages compared to a diesel-powered system:

- **Reduction in diesel consumption and associated CO_2-e emissions**
  This is because an electric-driven refrigeration unit is used to freeze the eutectic solution during charging, eliminating diesel fuel required for refrigeration.
- **Reduction in energy cost**
  Up to 86% of energy cost savings can be achieved by charging the eutectic system with off-peak grid electricity (Liu et al., 2012). Further reductions in cost and CO_2-e emissions can be achieved if the eutectic refrigeration system is charged using renewable electricity.
- **Low maintenance**
  Unlike a diesel-powered system, eutectic refrigeration is independent from the chassis and has fewer moving parts. Therefore, only very basic maintenance is required such as cleaning, lubricating and taking care of the refrigerant level.

Eutectic (PCM) plates

Figure 3. Eutectic refrigerated truck – view from back door.

2.2   Technologies enabling better performance

2.2.1   Refrigerants

Refrigerants with low global warming potential (GWP) have been used in refrigerated transport to phase out hydrofluorocarbon (HFC) refrigerants. These include:

- R452A

R452A (GWP of 2,139) is a non-flammable hydrofluoroolefin/hydrofluorocarbon (HFO/HFC) blend. It is now the refrigerant of choice in refrigerated transport to replace R404A (GWP of 3,922) and can help to reduce the carbon footprint of refrigerants by nearly 50%. Material testing results showed that R452A has similar material compatibility and chemical stability to R404A, indicating products utilising R452A have similar reliability to R404A products (Kujak & Schultz, 2018). Currently, trailer/intermodal and diesel driven single temperature trucks are rapidly transitioning from R404A to R452A with improved designs and reducing refrigerants by around 25% (Brodribb et al., 2021). The performance of a refrigeration system charged with R452A has demonstrated equivalent capacity and efficiency to a system charged with R404A (Kujak & Schultz, 2018).

- Natural refrigerants

Recently, natural refrigerants R290 (propane, GWP of 3) and R744 (carbon dioxide, CO_2, GWP of 1) have gained considerable attention because of their low environmental impact (Maiorino et al., 2021). Refrigeration systems using R290 have a higher COP of about 15-25% and 10-30% compared to R404A in medium and low temperature applications, respectively (Colbourne et al., 2016). This aligns with the result from an experimental study where a R290 refrigeration system had a 28.6% higher COP than R404A (Ramaube & Huan, 2019). Compared to R290, R744 has the advantage that it is non-flammable. The transcritical CO_2 refrigeration cycle, which has been utilised in stationary applications, has been introduced by Carrier Transicold for refrigerated containers.

2.2.2   Refrigeration system

Technologies used or being developed by refrigerated transport suppliers are summarised in Table 2.

- Battery Powered Refrigerated Vehicles

Thermo King, TKT HVAC Solution and Zanotti have already supplied a battery powered refrigeration unit on board an electric vehicle. This type of system has the benefit of being lightweight, low maintenance and low noise emissions. It is very suitable for urban area delivery. However, this battery powered system has only been designed for small trucks and vans requiring low cooling capacity.

- Carrier ECO-DRIVE Power Module

Carrier Transicold introduced a new generation of engineless transport refrigeration technology. The refrigeration unit is powered by the ECO-DRIVE power module and the operation process is shown in Figure 4. The hydraulic pump, connecting to the truck's power take-off motor, delivers electrical power to the refrigeration unit.

Table 2. Summary of technologies available/being developed by refrigerated transport suppliers.

Supplier	Technology (status)	Model	Type of vehicle	Cooling capacity[1]/weight	Source
Thermo King www.thermoking.com	Full-electric refrigeration unit (Available on market)	B-100, powered by vehicle's battery	small trucks and delivery vans in fresh applications	1 kW (fresh)	https://www.thermoking.com/na/en/road/trucks-and-vans/direct-drive-units.html
	Full-electric refrigeration unit for both electric and engine-powered vehicles (Available on market)	E-200, powered by vehicle's alternator	medium-size vans and trucks in fresh and frozen applications	1.377 kW (fresh) 0.791 kW (frozen)	
Carrier Transicold www.carrier.com	CO_2 refrigeration (Prototype testing under real conditions for 3 years)		Semi-trailer		https://www.carrier.com/carrier/en/worldwide/news/news-article/carrier_transicold_natural_refrigerant_trailer_mobiliteitsrai_show_simon_loos.html
	All-electric refrigeration unit with ECO-DRIVE power module (Available on market)	Vector HE19 Vector 1550 E (ECO-DRIVE25) ICELAND 11 Iceland 18 Twincool	Truck, trailer, drawbar		https://www.carrier.com/truck-trailer/en/uk/products/eu-truck-trailer/trailer/vector--he-19/
	All-electric refrigerated trailer system by using AddVolt's technology (Available on market)	Vector® eCool™	Trailer	9.8 kW (-20°C) 17.65 kW (0°C) 800 kg including battery	https://www.carrier.com/truck-trailer/en/uk/products/eu-truck-trailer/trailer/vector-ecool/
Bosch & Carrier Transicold	FresH$_2$ project, the hydrogen fuel cell refrigerated transport (Field testing in September 2021 in France)		Semi-trailers	30 kW fuel cell H$_2$ storage system: 350 bar & 10 kg;	https://www.carrier.com/truck-trailer/en/eu/news/news-article/fresh2-hydrogen-fuel-cell-refrigerated-transport-project--enters-road-testing-phase.html
Mitsubishi www.mhi-mth.co.jp	Electric driven refrigeration system, operated via 24V alternator and backup operation via 24V battery system, standby operation via 230V power supply. (Available on market)	TE 30 TE 30 Multi-Temp	Truck	1.17 kW (-20°C) 3.019 kW (0°C) 1.229 kW (-20°C) & 2.925 kW (0°C)	https://www.atrplus.com.au/cool-news-room/mitsubishi-te30-reefer-unit
TKT HVAC solution www.tkthvac.com	Battery powered electric van refrigeration unit (Available on market)	TKT-200E TKT-300E	Van	-5°C	https://www.tkthvac.com/products/van-refrigeration-units/electric-cargo-van-refrigeration-units/55.html
Zanotti www.zanotti.com	Battery powered electric van refrigeration unit (Available on market)	Z120	Van	0.55 kW (-20°C) 1.3 kW (0°C)	https://www.zanotti.com/zanotti-refrigerazione-mobile/refrigerazione-trasportata-con-batteria-zero-battery/

Note: 1. "fresh" and "frozen" refer to the temperature range of 0 – 4°C and -20 – -18°C, respectively.
2. Blank cell indicates that the information is not provided in the source.
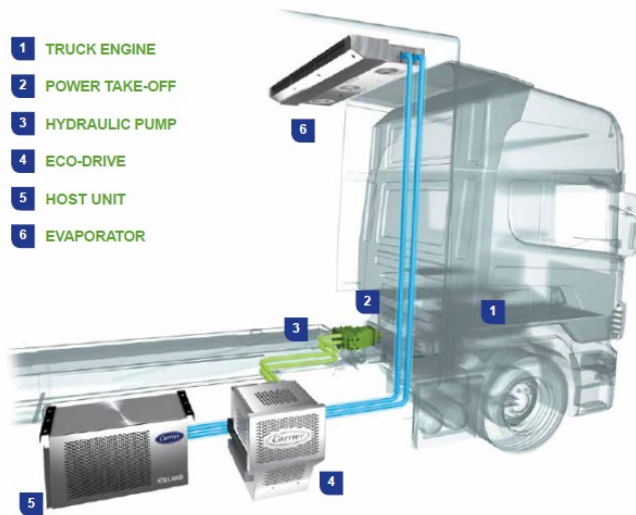
Figure 4. Schematic of ECO-DRIVE power module (Carrier Transicold, 2018).

- Carrier Vector® eCool™ Refrigerated Trailer System

In October 2021, Carrier Transicold launched the all-electric engineless refrigerated trailer system. Utilising AddVolt's engine-agnostic technology, Vector® eCool™ converts kinetic energy generated by the trailer into electricity, which is then stored in a battery pack to power the refrigeration unit, as illustrated in Figure 5. The battery pack has a total capacity of 19.2 kWh, weighs 325 kg and is capable of providing a maximum continuous discharge power of 19 kW. A full battery charge via the grid takes 2h.

Figure 5. Vector® eCool™ engineless refrigerated trailer system (Carrier Transicold, 2021a).

- Bosch & Carrier Transicold Hydrogen Fuel Cell Refrigerated Transport

The FresH$_2$® fuel cell project initiated by Bosch and Carrier Transicold, in collaboration with refrigerated vehicle builder Lamberet and temperature-controlled food transport specialist STEF, entered its road testing phase in France in early September 2021 (Carrier Transicold, 2021b, 2021c).

Figure 6. "FresH$_2$" hydrogen fuel cell refrigerated transport (Carrier Transicold, 2021b).

- Mitsubishi TE30/TE30 Multi-Temp Electric Transport Refrigeration Unit

Mitsubishi Heavy Industries Thermal Systems Ltd has launched an all-electric system. This system is driven by an engine powered 24V alternator during transportation of the produce. When the vehicle engine is turned off, the management system will automatically switch power source to the backup battery (24V). The battery can be charged by plugging in to a 230V power supply, also while the vehicle engine is running. The key components of this refrigeration unit are presented in Figure 7.
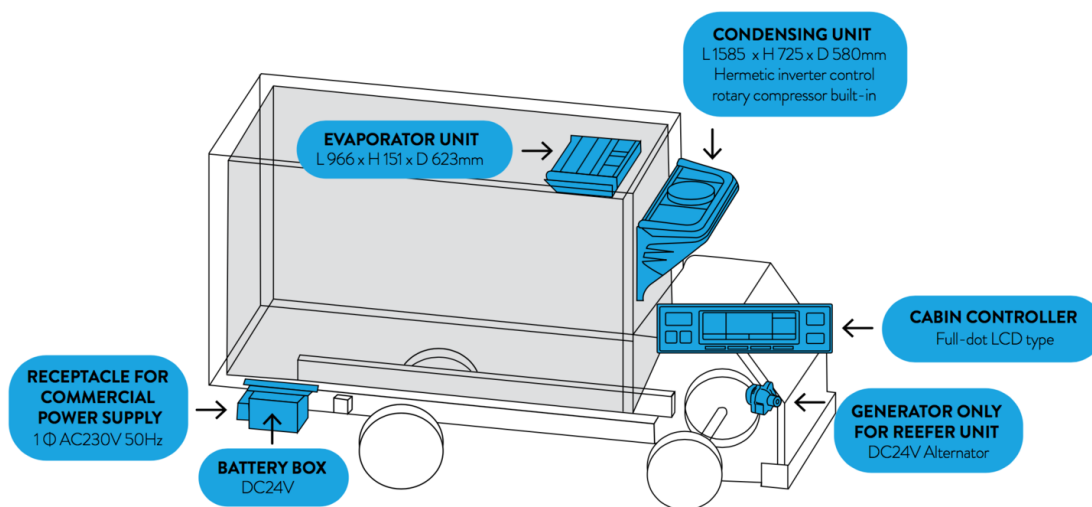
Figure 7. Mitsubishi TE30 electric system (Advanced Transport Refrigeration & AirConditioning, 2021).

2.2.3   Monitoring and control system

Temperature is the key factor that affects the shelf life of perishable foods. The proper control and management of temperature from farm through to customer is critical to ensure the food is in good quality and safe to eat. It will also contribute to a reduction in waste and energy consumption. An Australian Alliance for Energy Productivity (A2EP) report revealed that 10% of energy, costing $15 million, used in truck refrigeration can be saved by improving food condition monitoring in

Australia (A2EP, 2017a). However, there is only limited monitoring implemented in the Australian food cold chain.

Radio frequency identification (RFID) has been demonstrated in case studies in food cold chain management (Estrada-Flores & Tanner, 2008). An RFID system usually comprises a sensor, a tag and a reader to gather information from the tag wirelessly. Walmart has investigated the use of RFID and digital temperature recorders in its cold supply chain inventory tracking system (A2EP, 2017b). It allows Walmart to monitor and manage the effects of temperature conditions on perishable produce to decrease food spoilage and respond faster to equipment failure.

Remote real-time temperature monitoring already exists and has been used for high value and highly temperature sensitive products. With the falling cost of temperature monitoring and reporting technologies, real-time monitoring of food temperature is expected to become an industry standard within five years (A2EP, 2017a). As illustrated in Figure 8, a system to enable remote real-time temperature monitoring consists of the following elements:
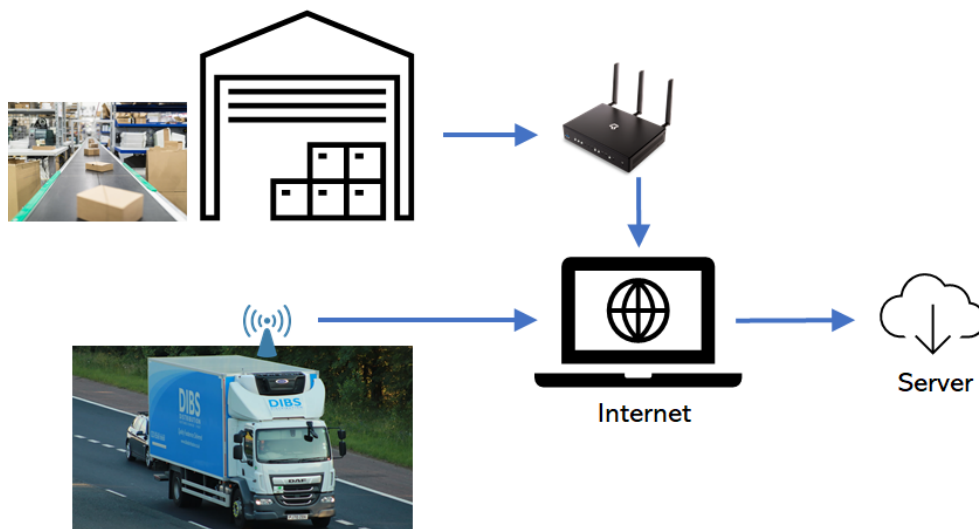
Figure 8. A real-time temperature monitoring system.

- Sensors

Low-cost sensors are commercially available to monitor temperature, humidity, and light (which indicates when doors are open or exposed to radiant heat). Pilots have indicated that at least 12 sensors per truck (ideally at least 1 sensor per pallet) are needed due to the large temperature variation in the space. It is suggested that placing much larger numbers of sensors for research/pilot purposes will help to determine the optimum numbers and locations of sensors required for alternative circumstances (A2EP, 2017a).

- Transmitters

Transmitters convert the measured temperature/humidity/light from the sensor into the signal and send it to the monitor/control device. They are usually packaged with a battery, sensors, and an aerial in a unit the size of a matchbox. The bulk cost is $10-15 each and the price is expected to further reduce.

- Communications network

IoT devices communicate over the network connection. The main constraint on ubiquitous low cost monitoring in Australia is the extent of low power wide area networks (LPWAN), but it is expected to be resolved within two years (A2EP, 2017a).

- Controllers

Wireless controllers allow remote monitoring of temperature and performance of the refrigeration unit in real time from devices such as smart phones or tablets via an app and hence remote managing the refrigeration unit by changing the set temperature.

2.2.4   Truck body

To increase payloads and reduce fuel consumption, it is necessary to use lightweight material for construction of the vehicle body. Truck bodies made of fibreglass, which is a strong and lightweight material, results in 20 to 30% less heat losses compared to truck bodies made of steel.

In Australia, currently there is no regulated insulation specification for walk-in cold rooms, refrigerated vehicles or cold storage facilities (Brodribb & McCann, 2020). The maximum width of refrigerated trucks in Australia and New Zealand is limited to 2.5m, compared to 2.6m in Europe and North America. Therefore, the insulation used by Australia and New Zealand refrigerated transport manufacturers has to be thinner. To achieve the same R value, better insulation material with a lower value of thermal conductivity is needed. Table 3 lists the thermal conductivities of several insulation material for cold storage (ASHRAE, 2018) .

Table 3. Thermal conductivity of cold storage insulation (ASHRAE, 2018).

Insulation	Thermal Conductivity [a] k, W/(m·K)
Polyurethane board (R-11 expanded)	0.023 to 0.026
Polyisocyanurate, cellular (R-141b expanded)	0.027
Polystyrene, extruded (R-142b)	0.035
Polystyrene, expanded (R-142b)	0.037
Corkboard [b]	0.043
Foam glass [c]	0.044

Note:
[a] Values are for a mean temperature of 24°C, and insulation is aged 180 days.
[b] Seldom used. Data are only for reference
[c] Virtually no effects from aging.

In 2021, the Australian Trucking Association has submitted recommendations to the Australian Government to increase the width of truck and trailer to 2.6 m to be consistent with international standards in Europe and North America (Australian Trucking Association, 2021). The thermal efficiency improvement of increasing wall insulation from the existing 2.5 m refrigerated vehicle (40mm insulation) to 2.55 m (65 mm insulation) and 2.6 m (90 mm insulation) is presented in Figure 9. The estimation is based on a 30°C difference between the internal and the outside temperature.
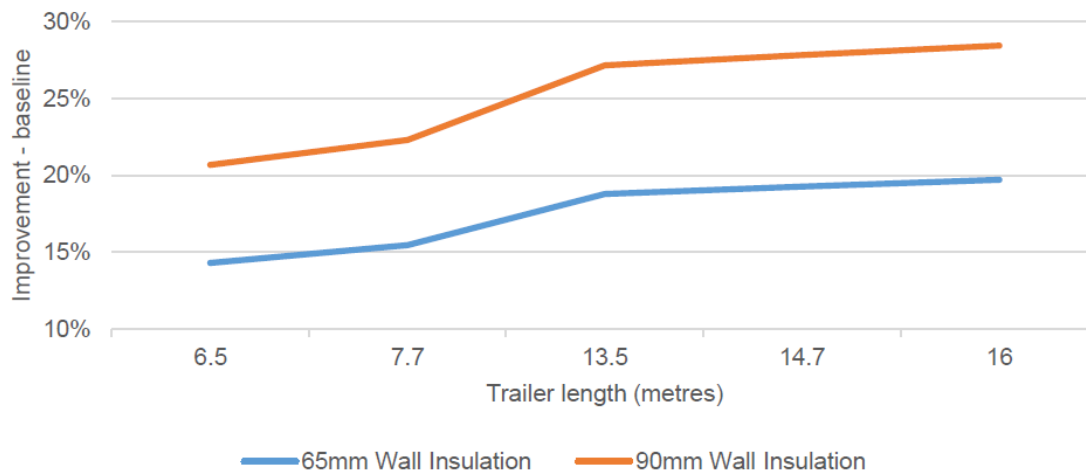
Figure 9. Thermal efficiency improvement by increasing the wall insulation from 2.5 m to 2.55 m (65 mm) and 2.6 m (90 mm) in a refrigerated vehicle (Australian Trucking Association, 2021).

Vacuum insulation panels (VIP), with an excellent thermal insulation property (thermal conductivity: 0.002 – 0.008 W/(m·K)), have been used as insulation for temperature-controlled packaging, refrigerators, freezers, refrigerated transport and insulated shipping containers. In conventional VIPs, a core material with high porosity and compressive strength is evacuated and sealed inside an envelope. Various materials commonly used as core materials include powders (e.g. fumed or pyrogenic silica, silica aerogel and expanded perlite), polyurethane and expanded polystyrene foams, glass fibre and hybrids (Resalati et al., 2021). The thermal conductivity of VIPs made from different core materials are summarised in Table 4.

Table 4. Thermal conductivity of VIPs with different cores (Resalati et al., 2021).

Core material	Thermal conductivity, W/(m·K)	Core material	Thermal conductivity, W/(m·K)
Fumed silica	0.0035 – 0.007	Aerogel	0.01 – 0.03
Phenolic foam	0.005	Polyurethane foam	0.005 – 0.007
Fibres (glass or wood)	0.001 – 0.009	Pyrogenic silica hybrid	0.0037 – 0.0103

2.3 Numerical modelling of transport refrigeration system

Computational Fluid Dynamics (CFD) tools such as ANSYS Fluent allow researchers to replicate simultaneous mass and heat transfer in refrigeration systems. In a refrigerated container, heat transfer occurs between the outside and inside environments including the food itself. It is important to maintain a uniform flow and temperature inside the container to keep the quality of the produce intact during the trip until arriving at the destination. Using CFD analysis, different designs of the refrigeration and/or PCM system can be examined to optimise the heat transfer area, air and temperature distribution. Building upon the recent knowledge shared in this area, a few relevant studies are discussed providing insights into the modelling of different refrigeration systems with PCMs.

Lafaye de Micheaux et al. (2015) used a wind tunnel to examine the infiltration flow rate through an opening door of a refrigerated truck. The results of the study showed an overall heat transfer coefficient of 0.576 W/m²·K for the insulated container. Results of a numerical study by Ben Taher et al. (2021) showed the benefit of PCM incorporated under the roof of a truck. When doors were open for 15 minutes, the inside temperature increased from 2°C to 11°C compared to the increase from 1°C to 17°C without PCM.

A numerical study by Kayansayan et al. (2017) investigated the impact of the length of cold air ejector inside a refrigerated truck with different aspect ratios; length/height (L/H). Results of the study showed the optimal injection velocity of 3.47 m/s, 6.94 m/s and 13.88 m/s for the L/H of 2.45, 3.33 and 5.32, respectively. The highest L/H showed the poorest performance in air circulation and temperature uniformity for different injection velocity, while L/H=3.33 demonstrated the highest performance at higher injection velocity.

From two numerical studies, Senguttuvan et al. (2021, 2020) found that directing the cold air from the refrigeration unit along the bottom of a refrigerated container (L=5.79 m, L/H=2.5) and return air to the top of the unit provides a higher heat transfer and temperature uniformity. Using different fan pressures of 50, 100 and 150 Pa showed a higher performance for 100 Pa compared with 50 Pa and a moderate improvement for 150 Pa compared with 100 Pa.

3. Eutectic Refrigeration

3.1   Literature review on phase change materials

This section presents potential phase change materials (PCMs), namely eutectic salts, to be used for cold thermal energy storage (TES) with melting/storage temperature between -40°C and 0.0°C. This will help the project team select suitable PCMs depending on the design and application of the cold TES system.

The desired thermophysical and chemical properties and economics of a potential subzero PCM candidate are (Oró et al., 2012; Yang et al., 2021):

- Thermophysical properties
  - Melting temperature in the desired operating temperature range
  - High latent heat of fusion per unit volume
  - High specific heat to provide additional significant sensible heat storage (in this case -40°C and 0.0°C)
  - High thermal conductivity of both solid and liquid phases
  - Small volume change on phase transformation
  - Small vapour pressure at operating temperature
  - Congruent melting of the PCM for a constant storage capacity of the material with each freezing/ melting cycle
  - Reproducible phase change
- Nucleation and crystal growth
  - High nucleation rate to avoid subcooling of the liquid phase during solidification, and to assure that melting and solidification process occurs at the same temperature
  - High rate of crystal growth, so that the system can meet the demand for heat recovery from the storage system
- Chemical properties
  - Complete reversible freeze/melt cycle
  - No degradation after a large number of freeze/melt cycles
  - No corrosiveness to the construction/encapsulation materials
  - Non-toxic, non-flammable and non-explosive
- Economics
  - Abundant
  - Available
  - Low cost
  - Easy recycling and treatment
  - Good environmental performance based on Life Cycle Assessment (LCA)

Eutectic phase change materials

A eutectic material which is a mixture of two or more species with a specific composition is the most common PCM. This kind of material has high thermal conductivity and density together with no phase separation.

Eutectic materials can be classified as either organic or inorganic. Table 5 summarises the specifications of each group. Eutectic water salt solutions with additives have been the most investigated subzero PCMs by researchers and commercial companies (Yang et al., 2021). For temperatures above 0°C, organic materials have been recommended. Melting temperature is one of the most important parameters for the selection of PCMs and designing the heat exchanger. Hence, the identification of the

eutectic temperature of the water-salt solution is the most important criteria that needs to be assessed by analysing the previously developed phase diagram of the hydrated salt (Oró et al., 2012). This helps to minimise the number of experiments for determining the melting temperatures of the eutectic salts, for the compositions which are away from the eutectic point. The studies on the eutectic NaCl-H_2O PCM supports the significance of the water-salt solution phase diagram (Han et al., 2006). Examples of inorganic salt solution phase diagrams can be found here ([Phase diagrams for binary salt solutions: Phase diagram](#)).

Table 5. General characteristic of organic and inorganic PCMs.

Group / specifications	Cost	Thermal conductivity	Latent heat of fusion	Energy density/volume	Volume change	Corrosiveness
Inorganic	Not expensive	High	High	Low	Insignificant	Corrosive / chemically unstable
Organic	Expensive	Low	low	High	Significant	Non-corrosive. Chemically stable

Table 6 summarises a list of inorganic subzero eutectic salt solutions and their thermal properties.

Table 6. Subzero PCMs evaluated by experimental method in previous studies (Oró et al., 2012).

PCM (wt. % of chemical in water solution)	Phase change temperature (°C)	Enthalpy (kJ/kg)	PCM (wt. % of chemical in water solution)	Phase change temperature (°C)	Enthalpy (kJ/kg)
40 $CuCl_2$	-40	166.17	19.5 NH_4Cl	-16	248.44-289
39.6 K_2CO_3	-36.5	165.36	36.8 K_2HPO_4	-13.5	189-197.79
17.1 $MgCl_2$	-33.6	221.88	30 $Na_2S_2O_3$	-11	219.86
21.01 $MgCl_2$	-33.5	36.30 (kJ/mol)	19.5 KCl	-10.7	253.18
30.5 $Al(NO_3)_3$	-30.6	131-207.63	32.2 $MnSO_4$	-10.5	213.07
34.6 $Mg(NO_3)_2$	-29	186.93	20 KCl	-10	284
39.4 $Zn(NO_3)_2$	-29	169.88	32.4 NaH_2PO_4	-9.9	214.25
32.3 NH_4F	-28.1	187.83-199.1	24.5 $Sr(NO_3)_2$	-5.75	243.15
40.3 NaBr	-28	175.69	16.95 $KHCO_3$	-5.4	268.54
$NaCl-NaNO_3$ (wt.% unknown)	-27	50-150	10 NaCl	-5	289
NaCl-KCl (wt.% unknown)	-23	260	20.6 $NiSO_4$	-4.15	258.61
21.5 KF	-21.6	225.2-227.13	19 $MgSO_4$	-3.9	264.42
22.4 NaCl	-21.2	222-235	12.7 Na_2SO_4	-3.55	284.95
$NaCl-Na_2SO_4$ (wt.% unknown)	-21	200	3.9 NaF	-3.5	309.2-314.09
25 $MgCl_2$	-19.4	223.1	9.7 KNO_3	-2.8	265.98
18 NaCl/5 super absorbent polymer /0.03 diatomite	-18.96	120.6	5.9 Na_2CO_3	-2.1	281-310.23
39.7 $(NH_4)_2SO_4$	-18.5	187.75-269	13.04 $FeSO_4$	-1.8	286.81
36.9 $NaNO_3$	-17.7	187.79	11.9 $CuSO_4$	-1.6	290.91
41.2 NH_4NO_3	-17.4	186.29	6.49 K_2SO_4	-1.55	268.8
35 $Ca(NO_3)_2$	-16	199.35			

Note: Blank cell indicates that the information is not provided in the source.

Enhancement of PCMs performance

Methods have been suggested to improve the performance of PCMs in terms of thermal conductivity, liquid leakage due to the phase change, subcooling and thermal stability.

One method is the addition of nanomaterials (such as metal particles, carbon fibre, graphite, and nanoparticle composites). More research has been conducted with organic PCMs. Limited attention has been given to the inorganic eutectic salt solution. The effect of nanoparticle deposits on the performance of some inorganic eutectic salt solutions has been investigated and the results are given in Table 7.

Table 7. A review on the subzero inorganic eutectic salt water solution PCMs with addition of nanomaterials to enhance the performance of PCMs.

PCM (composition in wt.%)	Nano-materials	Phase change temperature (°C)	Nucleating agent	Thickener	Subcooling degree (°C)	Latent heat of fusion (kJ/kg)	Thermal conductivity (W/(m·K))	Application	Year & Ref.
$BaCl_2$ (22.5)	TiO_2 with volume fraction of 1.13%	-8.5 (no change)			Basically eliminated	254.2 (decreased by 9.57%)	0.67 (improved by 16.74%)	Refrigeration in beer industry	Zhang et al. (2021)
$K_2HPO_4 \cdot 3H_2O$-$NaH_2PO_4 \cdot 2H_2O$-$Na_2S_2O_3 \cdot 5H_2O$ (6-6-6)	Modified expanded graphite (MEG)	-5.30 (fairly unchanged)	$Na_2B_4O_7 \cdot 10H_2O$ (1 wt%)		1.83	161.8 (decreased by 3.5% and 22% when compared with theoretical and experimental results, respectively)	8.90 (13.3 times that of eutectic salt solution)	Beer industry, air conditioning refrigeration, cold chain logistics	Xie et al. (2020)
$MgCl_2$ (23)	Multi-walled carbon nanotubes (MWCNTs 1 wt%) Considered as a corrosion resistance material	-34.54	1 wt% $CaCl_2$ and 0.25 wt% $Ca(OH)_2$	Xanthan gum (XG 0.5 wt%)	1.82	146.90 (decreased by 4.17%)	0.5344 (only 10% higher than pure eutectic solution due to the use of thickener forming a gel-like structure)	Cold Chain	Wu et al. (2020)

Note: Blank cell indicates that the information is not provided in the source.

Encapsulation and shape stabilisation methods have also been studied for the improvement of the performance of PCMs. However, these methods have not been investigated for subzero inorganic eutectic salt solutions (Zhang et al., 2021).

To combine the advantages of organic and inorganic PCMs, some studies have been conducted on organic-inorganic composite PCMs for cold TES applications (Li et al., 2021; Xing et al., 2022; Zhang et al., 2021). A ternary solution of organic salt of sodium formate (HCOONa) and inorganic salt of potassium chloride (KCl) in water identified from a previous study by Lu et al. (Lu et al., 2019), has been experimentally characterised (Xing et al., 2022). A mass fraction of 22% / 12% / 66% showed eutectic

characteristics with -23.8°C melting temperature and 257.2 kJ/kg. A 0.6 wt% of xanthan gum was suggested to supress phase separation and leakage while using nano-TiO₂ 0.6 wt% reduced supercooling by 67.9% (from 6.6°C to 2.6°C). The PCMs consisting of organic and inorganic water solution have been summarized in Table 8.

Table 8. A combination of organic and inorganic salt-water solution (Xing et al., 2022; Zhang et al., 2021).

Organic PCMs	Inorganic PCMs	Phase change temperature (°C)	Latent heat (kJ/kg)	Thermal conductivity (W/(m·K))	Application
22 wt.% sodium formate (-15.5°C; 282 kJ/kg)	12 wt.% KCl (-10.7°C; 253 kJ/kg)	-23.8	257.2		Cold storage
25% Ethylene glycol solution (-11°C; 96.8 kJ/kg)	15% NH_4Cl Solution	-16	212.8		Refrigerator
26 wt.% sodium formate (-14.8°C; 254.2 kJ/kg; 1.015 W/(m·K))	11 wt.% KNO_3	-18	279.1	1.182	Cold chain logistic
15 wt.% CH_3CH_2OH	25 wt.% NH_4Cl	-17.1	304		Freezer compartment of refrigerator
$C_6H_7KO_2$ (5 wt.%) $C_6H_7KO_2$ (25 wt.%) $C_{10}H_{14}N_2Na_2O_2H_2O$ (15 wt.%) HCO_2Na (5 wt.%) HCO_2Na (10 wt.%) HCO_2Na (15 wt.%) HCO_2Na (20 wt.%) HCO_2Na (22wt.%) HCO_2Na (25 wt.%)	KCl (25 wt.%) KCl (5 wt.%) KCl (15 wt.%) KCl (25 wt.%) KCl (20 wt.%) KCl (15 wt.%) KCl (10 wt.%) KCl (8 wt.%) KCl (5 wt.%)	-14 -18.6 -16.7 -23.6 -23.8 -23.8 -23.5 -23.8 -23.8	230.5 131.91 261.2 266.4 263.3 254.8 250.3 263.3		Preservation of frozen food

Note: Blank cell indicates that the information is not provided in the source.

Regarding corrosion, the assessment on sub-zero inorganic salt solutions has been given little attention.

Summary

Overall, experimental-based research for the selection of suitable sub-zero eutectic salt solutions is limited. Moreover, some potential salt solutions proposed in the literature are either not at their eutectic point or there is a disagreement about the eutectic composition reported. Therefore, future research needs to be directed towards the experimental validation of potential PCMs and identification of suitable PCMs with desired properties, and hence designing an effective eutectic refrigeration system for transport application. For salt solutions which are away from their eutectic points but worth investigating due to their potential of offering better performance, particular attention needs to be paid for refrigeration system design as the system needs to deal with both latent heat and sensible heat storage.

3.2   Characterisation and selection of phase change materials

Australian Food Cold Chain Logistic Guidelines require that chilled and frozen foods must be transported, stored and handled at temperatures never warmer than 5°C and -18°C, respectively (Australian Food and Grocery Council, 2017). Considering the efficiency of heat transfer when charging and discharging the eutectic system, PCM with melting temperatures in the range of -40°C up to 0°C is of interest for this project. After assessing the hazard level and economics of the chemicals, some promising candidates were selected from Table 6, as shown in Table 9.

Samples were prepared by mixing the pre-dried inorganic salt with water at desired weight ratios. The melting temperature (T_m), latent heat of fusion (ΔH_m) and specific heat capacity (C_p) of those samples were measured by using a PerkinElmer differential scanning calorimetry (DSC). The thermal conductivity (k) was measured by using a Trident Thermal Conductivity Analyzer (TCA). The density (ρ) is simply calculated by the ratio of mass to volume. All measurement results are summarised in Table 9. Latent heat energy density ($\Delta H_m/\rho$) vs. melting temperature of the PCM candidates are plotted in Figure 10.

Table 9. PCM candidates and experimental results.

PCM candidate	T_m (°C)	ΔH_m (kJ/kg)	C_p, solid (kJ/kg·K)	C_p, liquid (kJ/kg·K)	k @ 25°C (W/m·K)	P (kg/m³)	Note
PCM-33 #1	-32.7	180	1.60	3.00	0.52	1,085	Moderate energy density
PCM-33 #2	-32.7	218.8	1.55	2.90	0.51	1,153	*High energy density. Candidate #1*
PCM-33 #3	-32.7	155.6	1.64	3.73		1,178	Not good result
PCM-33 #4	-32.7	153.5					Not eutectic solution
PCM-32 #1	-31.96	96.6	1.3	2.55	0.52	1,292	Low energy density
PCM-32 #2	-32	149.6	1.7	2.8	0.52	1,349	Moderate energy density
PCM-28	-28	155.8	1.45	2.75	0.49	1,259	Moderate energy density
PCM-26	-25.84	169.4	1.25	2.42	0.49	1,386	*Moderate energy density. Candidate #2*
PCM-23	-22.8	229.4	1.42	2.94	0.53	1,192	*High energy density. Candidate #3*
PCM-21	-21	245.6	0.75	2.55	0.56	1,135	*High energy density. Candidate #4*
PCM-14	-14.2	75	1.5	1.6	0.58	1,277	Low energy density
PCM-10	-9.9	302.4	1.45	3.02	0.52	1,129	Very high energy density
PCM-3	-3.2	281	1.65	3.33	0.56	1,094	*Very high energy density. Candidate #5*
PCM-1	-0.74	254.9	0.67	3.93	0.6	1,097	High energy density
PCM1	0.83	327.06	1.65	3.73	0.58	1,075	Very high energy density

Note: Blank cell indicates that the sample has not been measured as it has been excluded based on previous testing. Differences in PCM-33 composition are confidential.
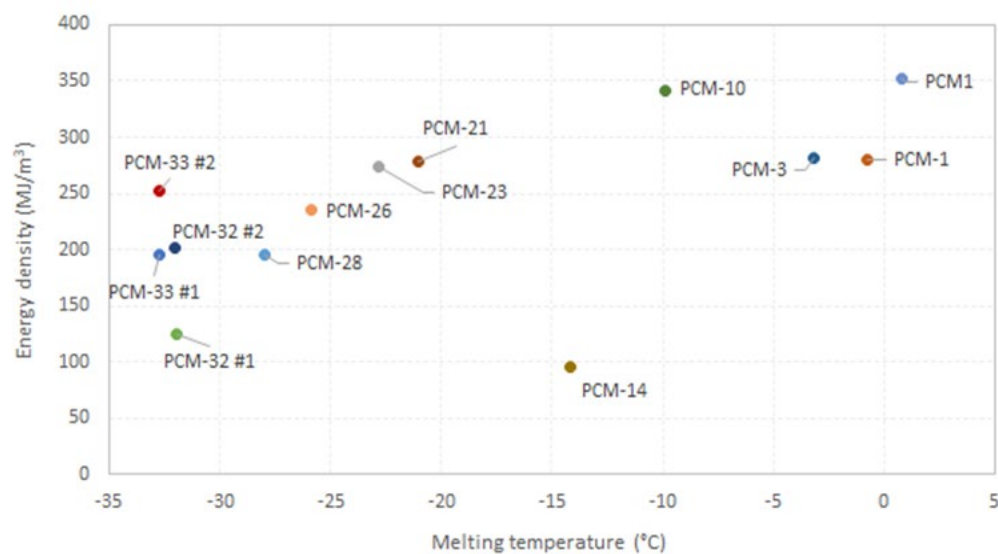
Figure 10. Latent heat energy density vs. melting temperature of the investigated PCMs.

3.3 Evaluation of existing eutectic refrigeration

Refrigerated trucks incorporating eutectic plates have been commercially available for over 20 years.

Our industry partner, Aldom Transport Engineering owns a recently retired eutectic refrigeration truck that was manufactured in 2003. The truck was used for delivering ice-creams during the day, while the eutectic plates were charged at night-time, taking about 12 hours with a charging power of about 3 kWh. The truck and the eutectic plates were examined, and a few conclusions were made:

1. The eutectic plates were made of stainless steel. It was observed that the steel was corroded by the eutectic solution, resulting in leakage (as shown in Figure 11). One plate was detached from the truck. The eutectic solution and refrigerant were carefully drained out of this plate. Then the metal plate was cut open. As can be seen from Figure 12, localised/pitting corrosion was found on the metal, which leads to the creation of small holes causing the leakage through the plate.
2. The plates and tubes were made of very thick steel, in particular the thickness of tube was approximately 3 mm. It is believed that much thinner material can be used to contain the eutectic solution if the selected material is more corrosion resistant. As a result, the weight of the plates can be reduced.
3. The eutectic plates cool the space by means of radiation and natural convection heat transfer. This "passive" heat transfer process is uncontrollable. If the space temperature rises due to door openings or high ambient temperature, the truck will be cooled down very slowly. This poses the risk of exposing the produce to high temperatures, which will increase the risk of food spoilage.
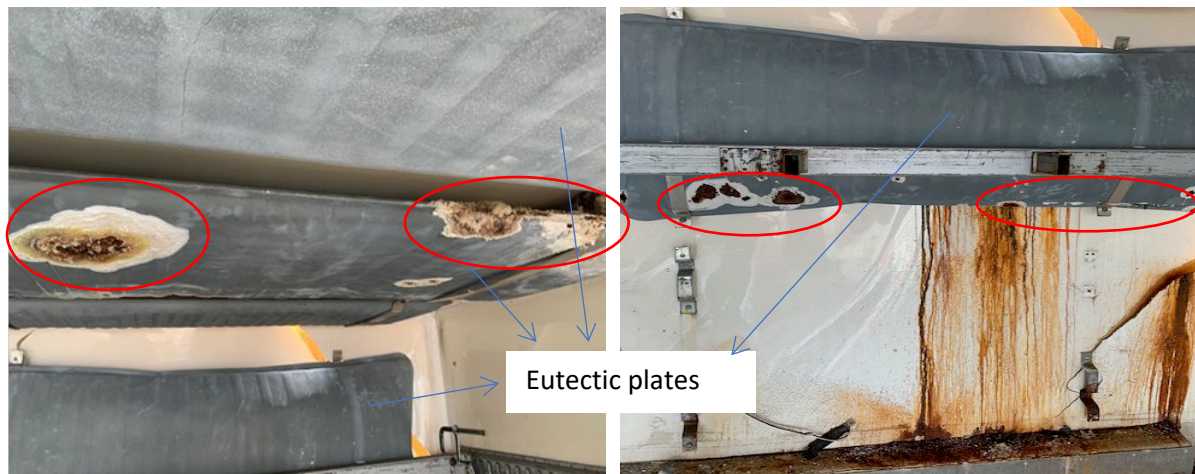
Eutectic plates

Figure 11. Corrosion on eutectic plates.

Figure 12. Interior of corroded eutectic plate.

4. Techno-economic Analysis

A techno-economic analysis has been conducted to evaluate four types of transport refrigeration systems for a medium-size refrigerated vehicle (dimensions of 4.2m (L) × 2.2m (W) × 1.9m (H)) used for both fresh and frozen produce delivery in Adelaide climate conditions (8 h from 9am to 5pm, 7 days per week). This is a two-compartment vehicle with frozen zone at -20°C in the front and chilled zone at 2°C in the back, accounting for 20% and 80% of the volume, respectively. The size of vehicle and operating conditions were selected by the industry partner Aldom to target supermarket customers.

The refrigeration systems under investigation are:

type i. Self-powered diesel VCR system (mostly common for medium to large vehicles).
type ii. Battery powered VCR system.
type iii. Eutectic refrigeration indirectly charged by an off-board electric refrigeration unit (as shown in Figure 13a).
type iv. Eutectic refrigeration directly charged by an on-board electric refrigeration unit (as shown in Figure 13b).
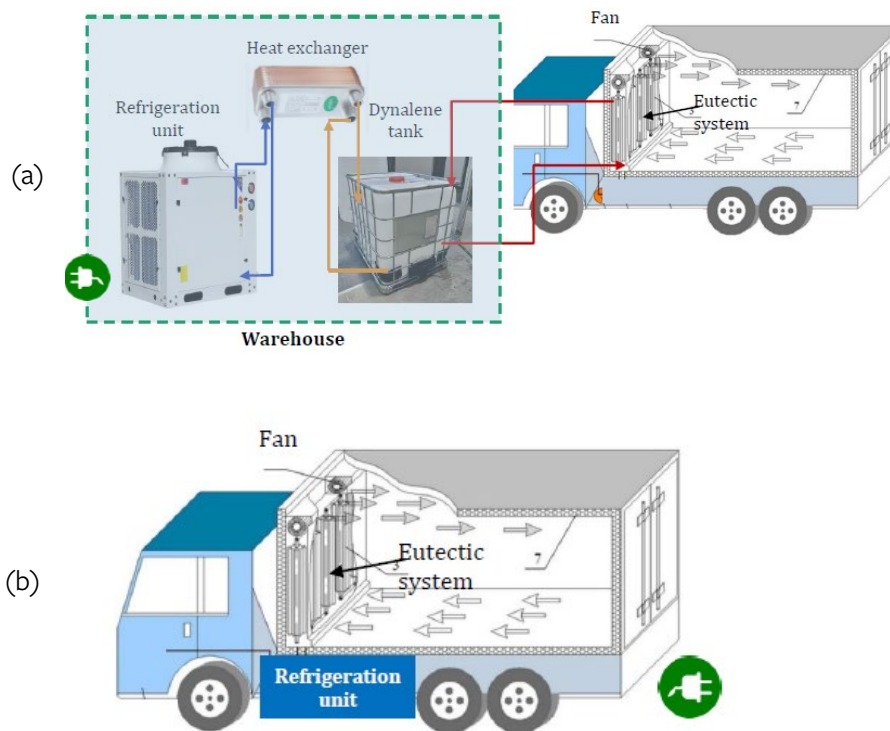
Figure 13. Schematic diagrams of type iii and type iv refrigeration systems under investigation.

Other than type i, all systems are operated using electricity, which reduces the energy cost and carbon emissions. Zero emissions could be achieved if the charging is correlated with renewable electricity generation. In both type iii and type iv, the eutectic system is charged by the refrigeration unit whenever the vehicle is not in use, which is generally at night since trucks are generally in use during the day (9am until 5pm, 7 days per week). With type i and ii, the refrigeration unit will supply the cooling as required to maintain the set temperature during the whole delivery period using diesel fuel and battery power respectively. The assumptions and estimated values used in this analysis are listed in Table 10.

Table 10. Assumptions and estimated values used in techno-economic analysis.

Vapour Compression Refrigeration Unit		Eutectic Refrigeration System	
COP (off-board, electric)	1.0 (Tassou et al., 2009)	Melting temperature of PCM (°C)	-32.7[5]
COP (on-board, diesel)	0.5 (Tassou et al., 2009)	Latent energy of fusion (kJ/kg)	218[5]
COP (on-board, electric)	0.5 (Tassou et al., 2009)	Effectiveness	0.8[6]
Cost of off board, electric driven refrigeration unit ($)	5,000[1]	Cost of PCM (*candidate#1*), including production ($/kg)	0.5[6] (large quantity production, e.g. > 10 tonnes)
Cost of on board, electric driven refrigeration unit ($)	6,000[1]	Volume of metal	10%[6]
Cost of on board, diesel driven refrigeration system ($)	12,000[1]	**General**	
Weight of electric driven refrigeration unit (kg)	125[1]	Cost of diesel ($/litre)	2.0
Weight of diesel driven refrigeration unit (kg)	413[2]	Cost of electricity ($/kWh) (off-peak)	0.275[7]
		Cost of installation	20% of the capital cost of the eutectic system
Battery System		**PV Panel[8]**	
Cost of packed battery ($/kWh)	220[3]	Power output (W) for 1m×1.7m panel	350
Specific energy (Wh/kg)	200[3]	Cost ($/kW)	600
Energy density (kWh/m³)	200[3]	Weight (kg/panel)	20
Cost of 6 kW on-board charger ($)	1,957[4]		

Note:
[1] Communication with Aldom.
[2] Thermo King T-90 Model T-590.
[3] Estimation based on the data from https://en.wikipedia.org/wiki/Lithium-ion_battery.
[4] https://www.thunderstruck-ev.com/tsm2500-x2-and-charge-controller.html
[5] Measured at UniSA.
[6] Based on experience at UniSA. Effectiveness = energy extracted from the storage system / total energy storage capacity.
[7] Based on AGL Standard Retail Contract Rates off-peak usage in South Australia from https://www.agl.com.au/-/media/aglmedia/documents/help/rates-contracts/market-contracts/2020/07/2020-my-pcp---agl-sa-elec-website-pricing-v7.pdf.
[8] https://gosolarquotes.com.au/solar-panel-dimensions/

The parameters to calculate the heat gain through doorways from air exchange are presented in Table 11. The R-value of the insulation material is 2.5 K·m²/W. Estimation of peak refrigeration load was made using the method in the *2018 ASHRAE Handbook – Refrigeration: Chapter 24 Refrigerated-Facility Loads* (ASHRAE, 2018). The outdoor design temperature for Adelaide is 42°C in the hottest month and this temperature was used to calculate the peak refrigeration load. It is assumed that the products

enter the frozen and chilled space at -20°C and 2°C, respectively, and the average heat of respiration rate of chilled products (1,500 kg) is 40 mW/kg. Heat gain from the fan motor is assumed to be 680 W. The effect of the weight on the total energy consumption is not included in the analysis but will be included in Phase 2 of the project.

Table 11. Door dimensions and door opening parameters.

	Chilled Zone	Frozen Zone
Width of door (m)	0.8	0.5
Height of door (m)	1.8	1
Number of doors	2	1
Number of openings per hour	4	2
Door open-close time (s/passage)	10	10
Time door stands open (s)	30	30
Doorway flow factor	0.8	0.8
Doorway protective device	curtain	curtain
Effectiveness of doorway protective device	0.5	0.5

4.1   Results

The peak refrigeration load is estimated to be 2,680 W, following the calculation procedure in *2018 ASHRAE Handbook – Refrigeration, Chapter 24: Refrigerated-facility Loads* (ASHRAE, 2018). In this case, the refrigeration load consists of transmission load (heat transfer into the refrigerated space through the truck envelope), product load (respiration heat from fresh product), internal load (heat produced by fan motors) and infiltration load (warm ambient air entering the refrigerated space). For the same size truck, Thermo-King recommends using its T-90 series of self-powered truck refrigeration unit model T-590, which has a cooling capacity of 4,543 W and 2,931 W at 2°C and -18°C, respectively, based on an ambient temperature at 37.8°C.

To calculate the total energy required during the daily delivery period and hence to estimate the amount of PCM required, an hour-by-hour load calculation was carried out using historical Adelaide climate data obtained from Lowa Environmental Mesonet (mesonet.agron.iastate.edu). The weather data between 1 January 2020 and 1 July 2022 was examined. The weather data from 9am to 5pm was used from 30th January 2020, which was the hottest day over the period. The hour-by-hour weather data and refrigeration load are presented in Figure 14.
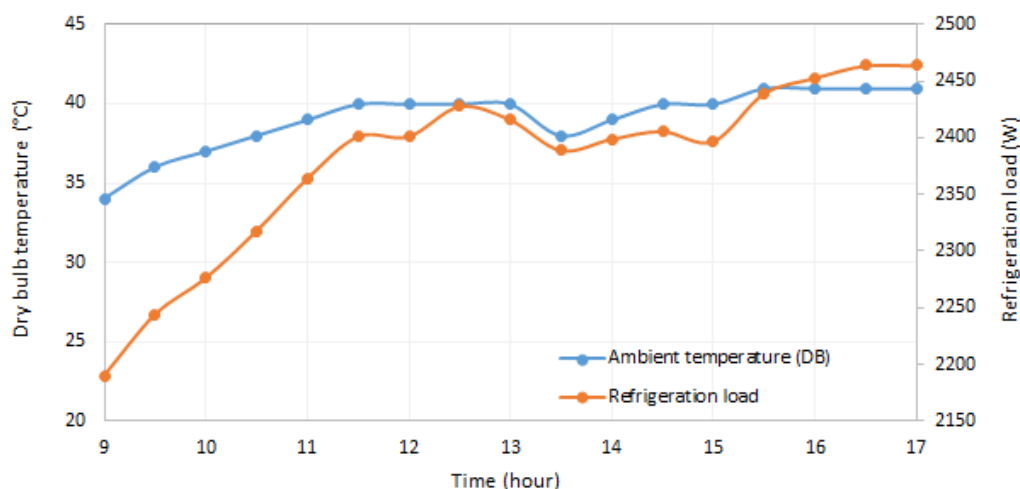
Figure 14. Hour-by-hour temperature and refrigeration load on the hottest day in Adelaide between 2020-2022.

The daily refrigeration energy is 20.22 kWh, thus approximately 360 kg of PCM is required assuming candidate #1 in Table 9 is used due to its high energy storage density. Due to the low thermal efficiency of the diesel combustion engine (~35%), 10.9 litres of diesel will be consumed on an extremely hot day, generating 29.21 kg CO_2-e emissions. If the eutectic system in type iii and type iv is charged using grid electricity in South Australia (with an emission factor of 0.43 kg CO_2-e/kWh), only 8.69 kg CO_2-e emissions will be produced. This represents 70% emissions reduction from a standard diesel-powered refrigeration option (type i).

The initial capital cost of the refrigeration system (CapEx), daily cost of energy (OpEx) (recharging using off-peak electricity), total cost of ownership over 10 years, weight of the four types of systems and daily CO_2-e emissions (from the refrigeration system, applied to the analysis in this chapter) were estimated using the values in Table 10. The results are presented in Figure 15. Total cost of ownership is determined by the CapEx, OpEx and discount rate (15% is used in this study). When calculating the OpEx, only the cost of diesel and electricity were considered. Other OpEx includes insurance, maintenance, repair, and employee training. It is worth noticing that the cost of maintenance for diesel-powered system is higher than that of the other types of system. Compared to the diesel-powered and electric-powered VCR refrigeration system, the eutectic refrigeration systems have the lowest cost of ownership, including CapEx and OpEx, and generate the least amount of CO_2-e emissions. The eutectic refrigeration system with an off-board electric refrigeration unit (type iii) requires infrastructure to be set up in the warehouse and it is more complex to assemble and operate. It is more suitable to a fleet of refrigerated vehicles that could share the same infrastructure. Therefore, the system with an on-board electric refrigeration unit (type iv) was selected as the first prototype to be constructed and tested on a single truck body in the Phase 2 of the project.
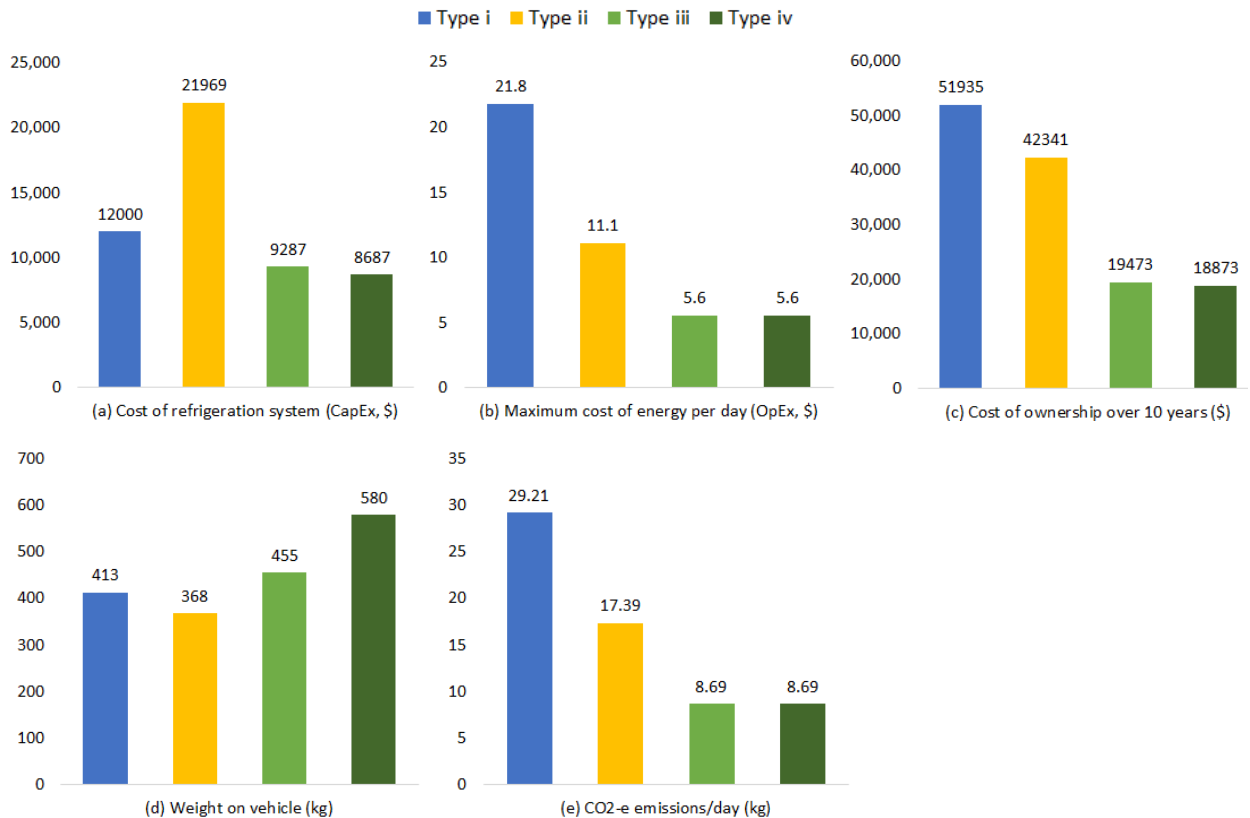
Figure 15. Cost, emissions and weight comparison of four types of refrigeration systems.

4.2   Impact of key parameters

- R-value

The R-value of the insulation panel has a significant impact on the transmission load. When the R-value is 2.5 K·m²/W, approximately half of the energy provided by the refrigeration system is for the transmission load. Peak refrigeration load and daily/transmission energy required at R-values of 2, 3, 4, 5 and 20 K·m²/W were calculated, and the results were plotted in Figure 16. A high R-value could be achieved by using VIP (in Section 2.2.4). For example, 50 mm VIP with an aerogel core (thermal conductivity of 0.01 W/(m·K)) and 100 mm VIP with glass fibre core (thermal conductivity of 0.005 W/(m·K)) has an R-value of 5 and 20 K·m²/W, respectively.
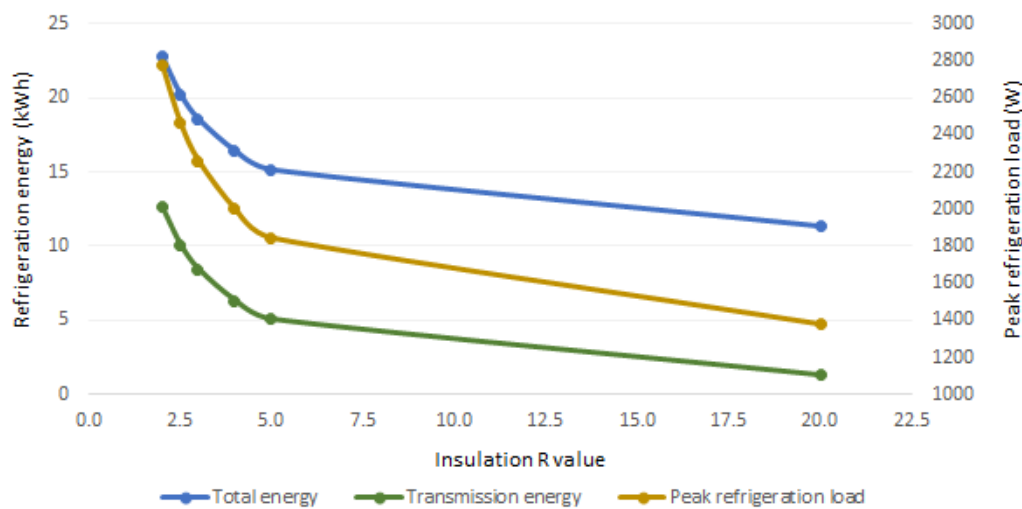
Figure 16. Refrigeration energy and peak load with different insulation R-values.

The amount of daily energy consumption (diesel for type i and electricity for the other three) and the daily CO_2-e emissions for the four types of refrigeration system were calculated and are shown in Figure 17. Both will drop by 25% and 43.7% if the insulation is improved from 2.5 K·m²/W to 5 K·m²/W and 20 K·m²/W, respectively, for all types. Compared to the diesel driven VCR system (type i), the battery driven VCR system (type ii) and eutectic refrigeration system (type iii and type iv) produce less CO_2-e emissions by 38.8% and 69.4% if they are charged by the South Australian grid, respectively, regardless of the R-value.

With improved insulation, the required amount of PCM and battery capacity will also be less. The weight of the battery powered VCR system and eutectic refrigeration system were presented in Figure 18. The battery system is lighter in most cases, but the discrepancy of weight between the battery and eutectic systems becomes smaller with increasing R-value. It is worth noting that when the R-value is 20 K·m²/W, the difference between type ii and type iii is small.
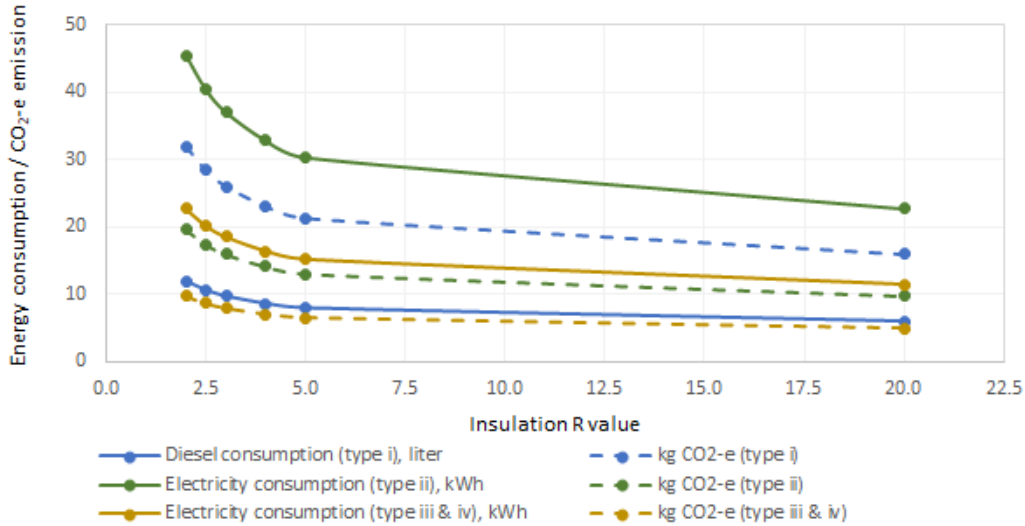
Figure 17. Energy consumption and CO_2-e gas emissions with different insulation R-values.
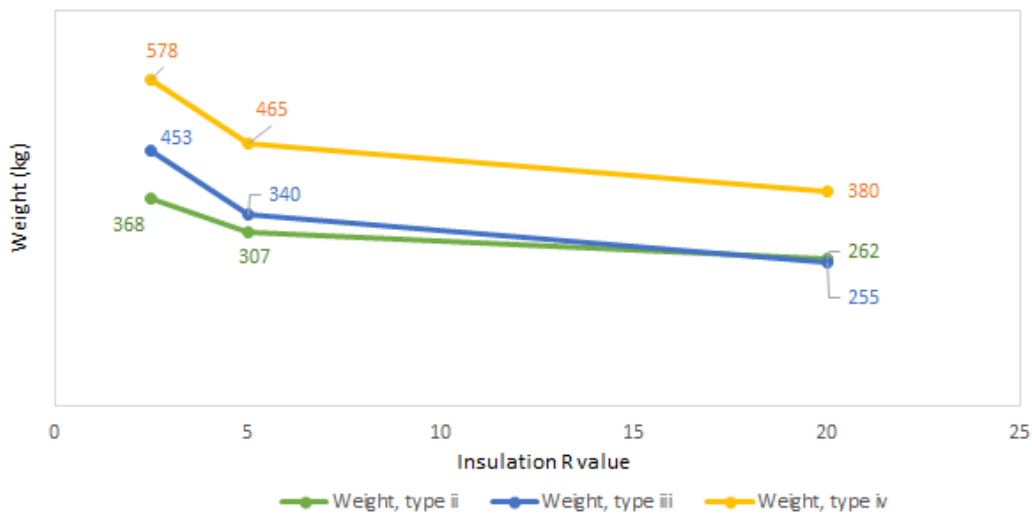
Figure 18. Weight of refrigeration system.

o   Specific energy of battery

Batteries are classified as lead-acid, nickel-based, ambient-temperature lithium, high-temperature, metal-air and flow batteries, as presented in Figure 19. Lithium-ion batteries have the advantages of high specific energy (Wh/kg) and energy density (Wh/l), long cycle life and high safety. Therefore, they not only dominate the battery market of portable electronics but also have widespread application in the booming market of automotive and stationary energy storage (Liu et al., 2022). Researchers (Liu et al., 2022) have recently reviewed the types of electric vehicle batteries currently available, which are summarised in Table 12. Based on the value range, four specific energies of low (100 Wh/kg), medium (200 Wh/kg), high (250 Wh/kg) and very high (300 Wh/kg) were selected to study the impact of specific energy on the weight of the battery powered VCR system (type ii). The weight of battery and refrigeration system at different specific energies are shown in Figure 20. The weight reduction is large (~50%) when the specific energy of the battery increases from 100 Wh/kg to 200 Wh/kg.
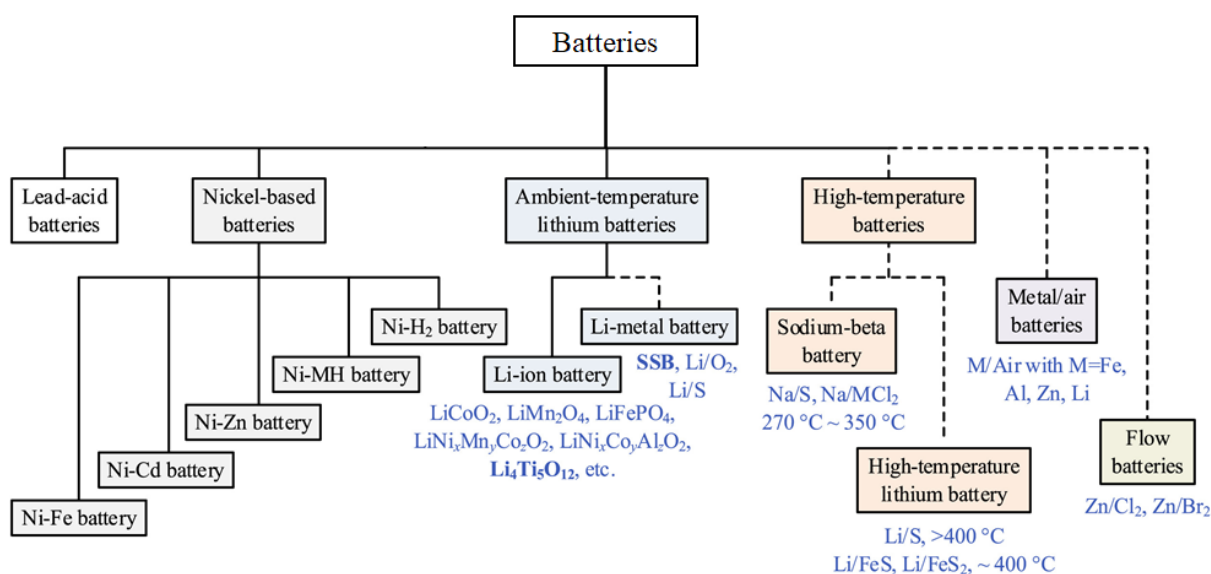
Figure 19. Classification of batteries (Liu et al., 2022).

Table 12. Critical survey of electric batteries (Liu et al., 2022).

Types		Overall chemical reactions	Specific energy (Wh kg^{-1})	Specific power (W kg^{-1})	Life cycle	Pros	Cons	Examples and vehicle applications
Lead–acid		$Pb + PbO_2 + 2H_2SO_4 \leftrightarrow 2PbSO_4 + 2H_2O$	30~50	150~200	400~800	Low cost, good performances in low and high temperatures	Low energy efficiency, low specific energy, memory effect	**VRLA:** Ford Ranger, Chrysler Voyager, Suzuki Alto
Nickel-based	Ni–Fe	$3Fe + 8NiOOH + 4H_2O \leftrightarrow 8Ni(OH)_2 + Fe_3O_4$	35~80	150~450	800~2000	Low cost, high specific power	Low energy efficiency, low specific energy	**Ni–MH:** Toyota RAV4L, Honda EV Plus, Peugeot 106
	Ni–Cd	$2NiOOH + 2H_2O + Cd \leftrightarrow 2Ni(OH)_2 + Cd(OH)_2$						
	Ni–Zn	$2NiOOH + 2H_2O + Zn \leftrightarrow 2Ni(OH)_2 + Zn(OH)_2$						
	Ni–MH	$MH + NiOOH \leftrightarrow M + Ni(OH)_2$						
	Ni–H$_2$	$2NiOOH + H_2 \leftrightarrow 2Ni(OH)_2$						
Ambient-temperature lithium	Li-ion	[a]$LiYO_2 + C \leftrightarrow Li_xC + Li_{1-x}YO_2$	120~300	200~450	600~>3000	High energy efficiency, high specific power, long life cycle	High cost (moderate), fire hazard (reliability)	**Li-Ion:** Tesla 3, BMW i3, Nissan Leaf
	Li-metal	[b]$xLi + M_yB_z \leftrightarrow Li_xM_yB_z$						
Sodium-beta	Na/S	$2Na + xS \leftrightarrow Na_2S_x$	115~200	120~250	800~2000	High energy efficiency, high specific energy	High operating temperature, safety concern, high cost	**Na/NiCl$_2$:** BMW AG, Mercedes-Benz Vito
	Na/MCl$_2$	$2Na + MCl_2 \leftrightarrow 2NaCl + M, (M = Ni, Fe)$						
High-temperature lithium	Li/FeS	$2Li-Al + FeS \leftrightarrow Li_2S + Fe + 2Al$	130~180	240~400	1000~1200			–
	Li/FeS$_2$	$2Li-Al + FeS_2 \leftrightarrow Li_2\,FeS_2 + 2Al$						
Metal/Air		$4M + nO_2 + 2nH_2O \leftrightarrow 4M(OH)_n, (M = Li, Zn, Al, Fe)$	75~250	100~200	300~800	Low cost, high specific energy, convenient refueling	High cost, low specific power, narrow operating temperature window	**Zn/Air:** Mercedes-Benz MB410, GM-Opel Corsa Combo
Zinc/Halogen	Zn/Br$_2$	$Zn + Br_2 \leftrightarrow Zn^{2+} + 2Br^-$	65~75	60~110	200~400	Refuel liquid, low cost	Frequency maintenance, low specific energy and power, high cost	**Zn/Br$_2$:** Fiat Panda, Hotzenblitz EV, Toyota EV-30
	Zn/Cl$_2$	$Zn + Cl_2 \leftrightarrow Zn^{2+} + 2Cl^-$						

[a]$LiYO_2$ nominally represents $LiCoO_2$, $LiNiO_2$, $LiMn_2O_4$ and $Li_4Ti_5O_{12}$.
[b]M_yB_z is the transition metal material.
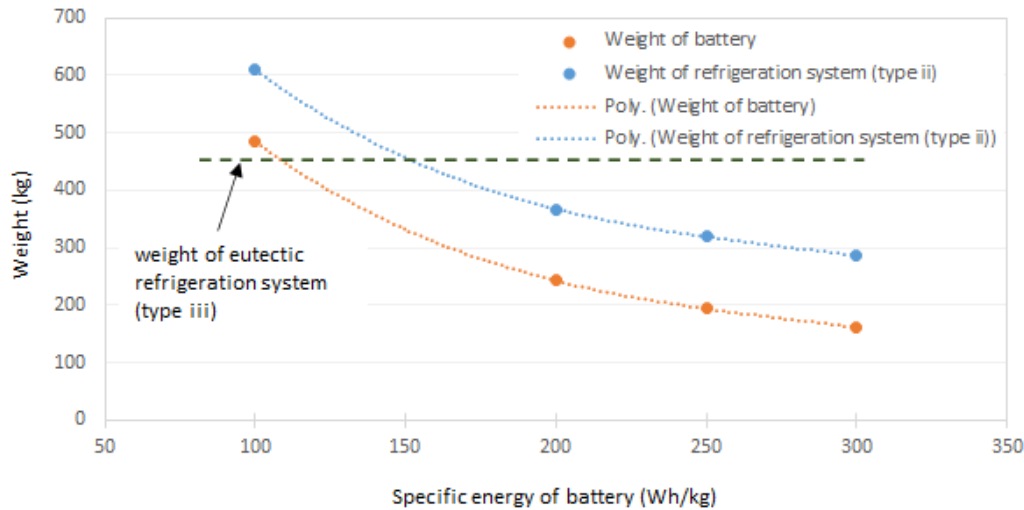
Figure 20. Weight of battery and refrigeration system.

  o Cost of battery

Since 2010, the price of batteries has fallen by about 89%. The current cost of lithium-ion per kWh is AUD$216 (US$137), which is predicted to drop to AUD$92 (US$58) by 2030 (Gaton, 2021) (US$1 = AUD$1.58). König et al. (2021) have given the range of battery pack costs (€/kWh) in Figure 21, with the numbers after year 2020 being the forecast. The current cost is already at the lower end in the range, therefore, the minimum costs in years 2024, 2026, 2028 and 2030 (1€/kWh = 1.5 AUD$/kWh) were selected for this analysis (red dots on Figure 21). The CapEx cost of battery powered VCR system (type ii) and battery pack were estimated and plotted in Figure 22. With the falling cost of batteries, the battery powered refrigeration system will gradually become cheaper over time. However, it will always be more expensive than the eutectic refrigeration system as long as the cost of battery is higher than AUD$2.1/kWh.
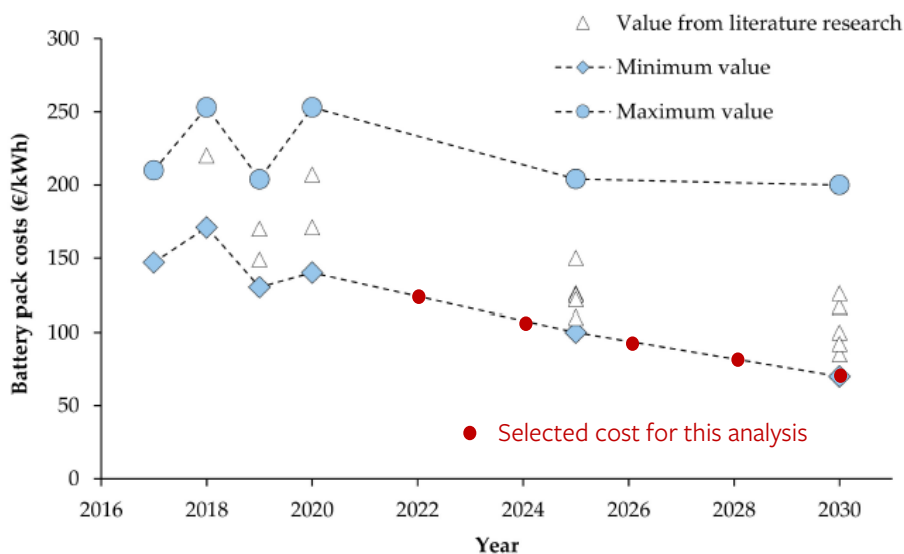
Figure 21. Costs of battery pack (no distinction made between cell types) (König et al., 2021).
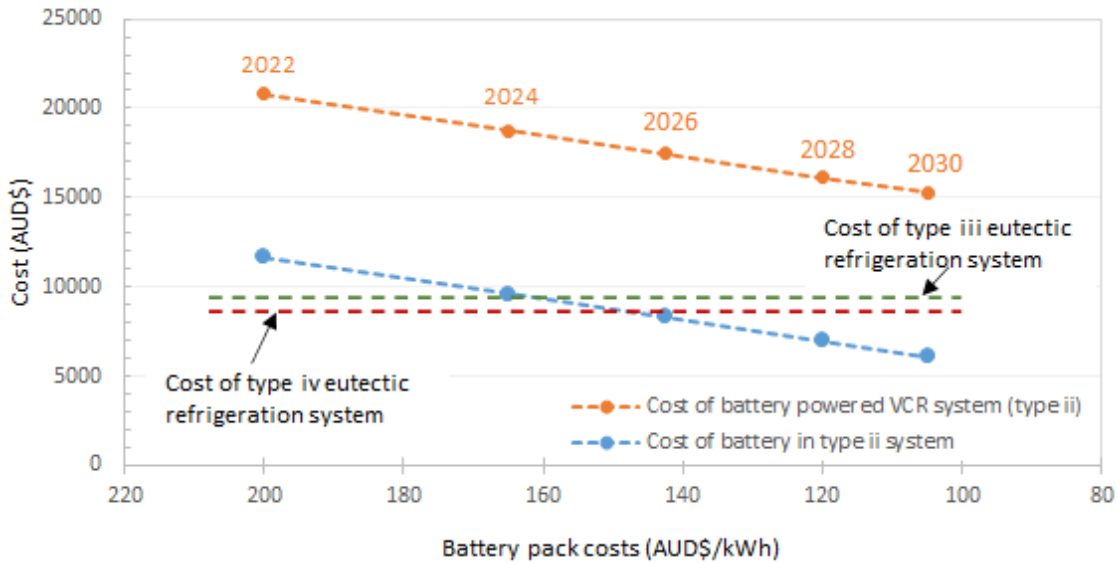
Figure 22. CapEx cost of battery pack and battery powered VCR system (type ii).

  o   Sensitivity analysis

A sensitivity analysis has been carried out to study the impact of key parameters on the cost of refrigeration system (CapEx), cost of energy (OpEx), total cost of ownership over 10 years, weight of refrigeration system (on vehicle) and CO_2-e emissions for the four types of refrigeration systems. The parameters investigated in this analysis include: COP of the refrigeration unit used in product delivery, COP of the refrigeration unit used for charging the eutectic system, insulation R-value ($K \cdot m^2/W$), specific energy of battery (Wh/kg), latent heat of fusion of PCM (kJ/kg), cost of battery ($/kWh), cost of refrigeration unit ($), cost of on-board charger ($, for battery-powered refrigeration system), cost of secondary heat exchanger ($, for type iii eutectic refrigeration system) and discount rate. The values of those parameters were varied by ±20%. Changes were made one parameter at a time, keeping all other parameters fixed to their baseline values in Table 10. The results obtained (CapEx, OpEx per day, cost of ownership, CO_2-e emissions per day and weight of on-board refrigeration system) were compared with the results from the baseline case presented in Figure 15. The results are listed in Table 13.

Several findings can be concluded:

  o   CapEx: the COP of the refrigeration unit and cost of battery are the two most critical variables that affect the CapEx of battery-powered refrigeration systems (type ii), while the insulation R-value and cost of the refrigeration unit has less impact. The CapEx of eutectic systems is influenced more by the cost of the refrigeration unit than the insulation R-value, latent heat of fusion of the PCM and the cost of secondary heat exchanger (type iii only).
  o   OpEx and CO_2-e emission: a decrease of 20% in COP for the refrigeration unit and R-value implies an increase of 25% and 12.5% of OpEx & CO_2-e emissions for all types of refrigeration systems, respectively. An increase of 20% in COP and R-value will lead to a decrease of 16.7% and 8.3% of OpEx & CO_2-e emissions, respectively.
  o   Cost of ownership: same as the CapEx and OpEx, the cost of ownership is affected primarily by the COP of the refrigeration unit regardless of the type of system, followed by the R-value and discount rate for type i and CapEx for types ii-iv, respectively.

o   Weight: compared to the R-value, the COP of the refrigeration unit has more influence on the weight of the battery-powered refrigeration system. If the latent heat of fusion of the PCM is 20% more than that of PCM candidate #1, the weight of the eutectic refrigeration system type iii and type iv can be reduced by 15% and 11.8%, respectively.

Table 13. Effect of key parameters on the results.

Effect of key parameters on CapEx			Type i		Type ii		Type iii		Type iv	
COP of RU	-20%	20%	-	-	14.6%	-9.7%	-	-	-	-
R-value	-20%	20%	-	-	7.3%	-4.8%	1.9%	-1.4%	2.0%	-1.5%
CapEx: cost of battery per kWh	-20%	20%	-	-	-11.7%	11.7%	-	-	-	-
CapEx: cost of RU	-20%	20%	-20%	20%	-6.6%	6.6%	-12.9%	12.9%	-16.6%	16.6%
CapEx: cost of on-board charger	-20%	20%	-	-	-1.8%	1.8%	-	-	-	-
CapEx: cost of secondary heat exchanger	-20%	20%	-	-	-	-	-3.9%	3.9%	-	-
Latent heat of fusion of PCM	-20%	20%	-	-	-	-	3.2%	-3.2%	3.4%	-3.4%
Effect of key parameters on OpEx			**Type i**		**Type ii**		**Type iii**		**Type iv**	
COP of RU	-20%	20%	25.0%	-16.7%	25.0%	-16.7%	25.0%	-16.7%	25.0%	-16.7%
R-value	-20%	20%	12.5%	-8.3%	12.5%	-8.3%	12.5%	-8.3%	12.5%	-8.3%
Effect of key parameters on cost of ownership			**Type i**		**Type ii**		**Type iii**		**Type iv**	
COP of RU	-20%	20%	19.2%	-12.8%	19.6%	-13.1%	13.1%	-8.8%	13.5%	-9.0%
Latent heat of fusion of PCM	-20%	20%	-	-	-	-	1.5%	-1.5%	1.6%	-1.6%
R-value	-20%	20%	9.6%	-6.4%	9.8%	-6.5%	7.5%	-5.0%	7.7%	-5.2%
Discount rate	-20%	20%	9.7%	-8.0%	6.1%	-5.0%	6.6%	-5.5%	6.8%	-5.6%
CapEx	-20%	20%	-4.6%	4.6%	-10.4%	10.4%	-9.5%	9.5%	-9.2%	9.2%
Effect of key parameters on CO_2-e emission			**Type i**		**Type ii**		**Type iii**		**Type iv**	
COP of RU	-20%	20%	25.1%	-16.6%	25.0%	-16.7%	25.1%	-16.6%	25.1%	-16.6%
R-value	-20%	20%	12.5%	-8.3%	12.5%	-8.3%	12.5%	-8.3%	12.5%	-8.3%
Effect of key parameters on weight			**Type i**		**Type ii**		**Type iii**		**Type iv**	
COP of RU	-20%	20%	-	-	16.4%	-11.1%	-	-	-	-
Latent heat of fusion of PCM	-20%	20%	-	-	-	-	20.2%	-15.0%	15.9%	-11.8%
R-value	-20%	20%	-	-	8.2%	-5.6%	12.0%	-8.7%	9.4%	-6.8%

4.3   Projection of CO_2-e emissions by 2035

In order to predict the amount of refrigeration-related CO_2-e emitted by refrigerated vehicles, a number of assumptions were made:

o   The stock of refrigerated vehicles increased dramatically from 21,150 in 2009 to 45,100 in 2018 (Brodribb & McCann, 2020; Brodribb et al., 2021; Mark Ellis & Associates Pty Ltd, 2009). No recent data after 2018 was found. It is assumed the total stock will keep rising at a similar rate, as shown by the solid green line in Figure 23.

o   As described in Table 1, diesel-powered truck refrigeration units are classified into three categories depending on the vehicle size. It is assumed the medium-size vehicle investigated in this work represents the average size, which has been applied to the whole stock, along with its

working conditions for 365 days per annum. Thereby, the amount of CO_2-e was calculated and considered as the baseline case (solid red line in Figure 23). These assumptions will be investigated in the next phase of the project.

o This project hopes to develop a new and improved eutectic refrigeration system by 2024. It is assumed that this product will start penetrating the market with a linear penetration rate of 9.1%. Thus, by 2035, this product is assumed to account for 15% of the market, the rest of which will likely still be dominated by diesel-powered refrigeration (indicated by the dotted green line in Figure 23). The same penetration rate was applied to the electric-powered refrigeration (type ii).

o Electricity is assumed to have an emission factor of 0.63 t CO_2-e/MWh (Scope 2 emissions), averaging the emission factors of all the states/territories (Clean Energy Regulator, 2022). This was applied to calculate the amount of CO_2-e by charging the battery (type ii) or the eutectic system (type iii and iv) by the grid. A standard emission factor of 0 was applied if those systems would be charged by electricity from renewable sources, such as from solar PV and wind power.
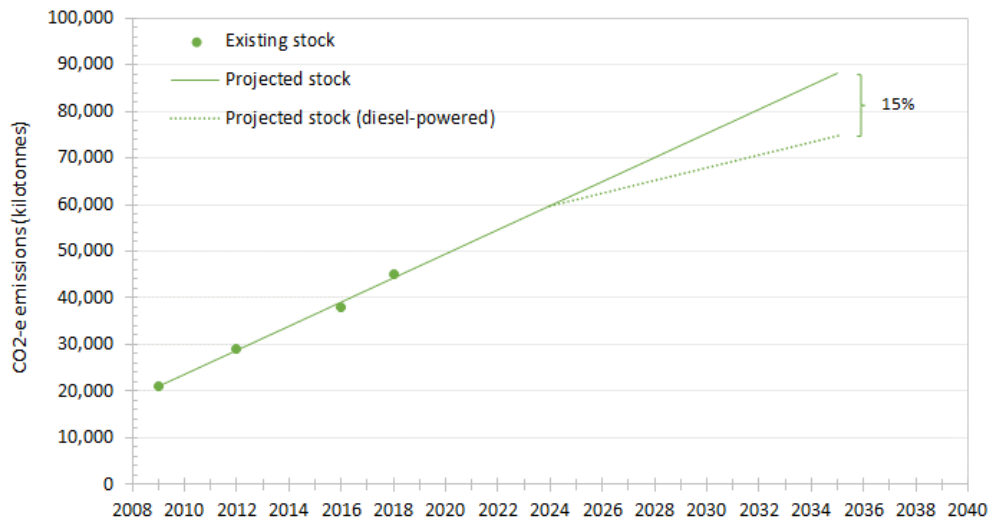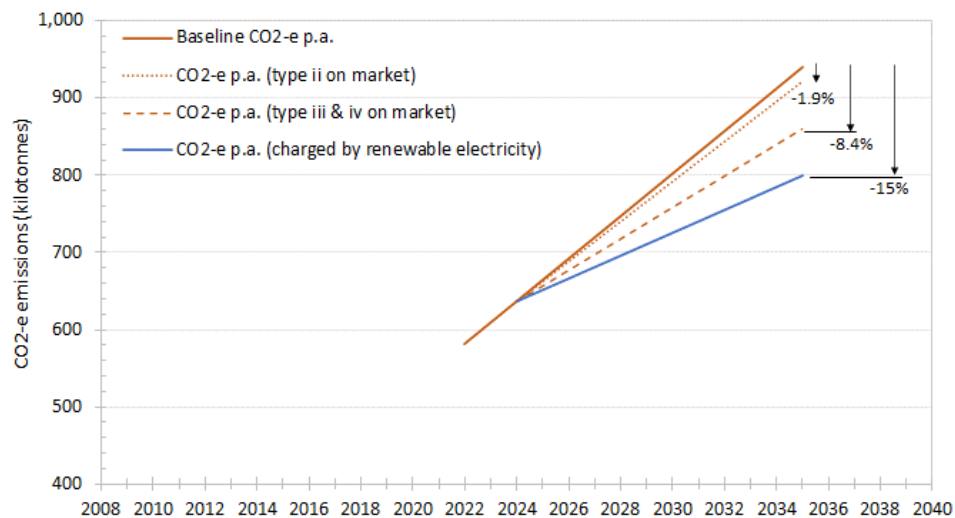
Figure 23. Projection of stock of refrigerated transport and CO_2-e emissions by 2035.

The predicted amount of CO_2-e emissions is presented in Figure 23. Four scenarios were considered in this analysis: (1) baseline, in which all the transport refrigeration systems are powered by diesel engines; (2) battery-powered VCR system will take up the market; (3) eutectic refrigeration systems will take up the market and (4) the battery-powered and eutectic refrigeration systems are charged by electricity from renewable sources while they are charged by grid electricity in scenarios (2) and (3). In the baseline case with only diesel-powered refrigeration units, CO_2-e emissions are predicted to increase dramatically and reach 940 kilo tonnes in 2035. Compared to diesel-powered refrigeration, eutectic (type iii or type iv) and battery-powered refrigeration technologies (type ii) could achieve a CO_2-e reduction of 56.3% and 13.6% for a single vehicle, respectively. Accordingly, those two technologies will contribute to a CO_2-e reduction of 79.4 kilo tonnes (8.4%) and 17.8 kilo tonnes (1.9%) by 2035, respectively. Under a scenario where charging is accomplished by using renewable electricity, a reduction of 15% could be achieved.

4.4   Conclusions

The following conclusions can be drawn from the techno-economic analysis:

- Benefiting from the higher COP of the refrigeration unit in colder night-time temperatures, eutectic refrigeration systems of types iii (off-board electric VCR system) and iv (on-board electric VCR system) have the lowest energy consumption and operating cost. Diesel consumption is high in the type i system (diesel-powered refrigeration) due to the very low efficiency of the diesel engine (~35%) and low COP of the refrigeration unit.
- Compared to the diesel driven VCR system (type i), the battery driven VCR system (type ii) and eutectic refrigeration systems (type iii and type iv) produce less CO_2-e emissions by 39% and 69% respectively. This assumes they are charged from the grid in South Australia.
- Improved insulation will allow for smaller and lighter refrigeration systems. The weight difference between the battery and eutectic system becomes smaller with increasing R-value.
- When the specific energy of a battery is greater than about 150 Wh/kg, battery-powered VCR systems is lighter than the eutectic refrigeration system as indicated in Figure 20.
- Even though the price of batteries has dropped by 89% over the last 10 years, the battery-powered refrigeration system (type ii) is still the most expensive option, followed by the diesel system. Eutectic refrigeration has a cost advantage over the other two systems; however, it adds extra weight on the vehicle. It will slightly increase the energy consumption for driving the vehicle.
- The amount of the CO_2-e emissions estimated in this report only accounts for the emissions from the refrigeration system, not from powering the vehicle. However, the heavier the refrigeration system, the more energy will be needed for driving the vehicle, leading to a larger amount of CO_2-e emissions. This research did not study the effect of the weight on the total energy consumption and CO_2-e emissions of the vehicle, which will be investigated in the Phase 2 of the project.
- The eutectic refrigeration system with an on-board electric refrigeration unit (type iv) will be further studied and a prototype will be constructed and tested in the Phase 2 of the project.

Although eutectic refrigeration systems have the advantages of low cost of ownership, including CapEx and OpEx, compared to battery-driven vehicle refrigeration systems, the commercial eutectic vehicle has the shortcomings of ineffectiveness in its thermal performance due to door openings as well as being too heavy. The problems stem from the design in regard to containment and location of the PCM, as well as the type of PCM used. This project addresses these problems by developing high performing PCM(s) in Chapter 3 and a new design of eutectic system in Chapter 5.

5. Concept Design and Numerical Simulation

5.1 Concept design of innovative eutectic refrigeration unit

To overcome the shortcomings of the existing commercial product, a novel eutectic refrigeration system needs to be designed. Unlike the commercial eutectic truck where the PCM plates are distributed under the roof and on the front of the refrigerated space as shown in Figure 4, in the new design the PCM is centralised and all the PCM containers are assembled in one case that is located in the front of the space, as illustrated in Figure 24. Also, the system used fan-driven forced convection of the air to ensure more uniform temperature distribution. A commercially available eutectic refrigerated truck was used as a base to calculate the heat transfer area and the weight of PCM needed. This vehicle has an internal dimension of 5.4 m length by 2 m width by 1.57 m height. To enable frozen food delivery for 8 hours, seven eutectic plates are installed with a total amount of PCM of about 450 kg (estimated) and a total plate heat transfer area of 17 m².
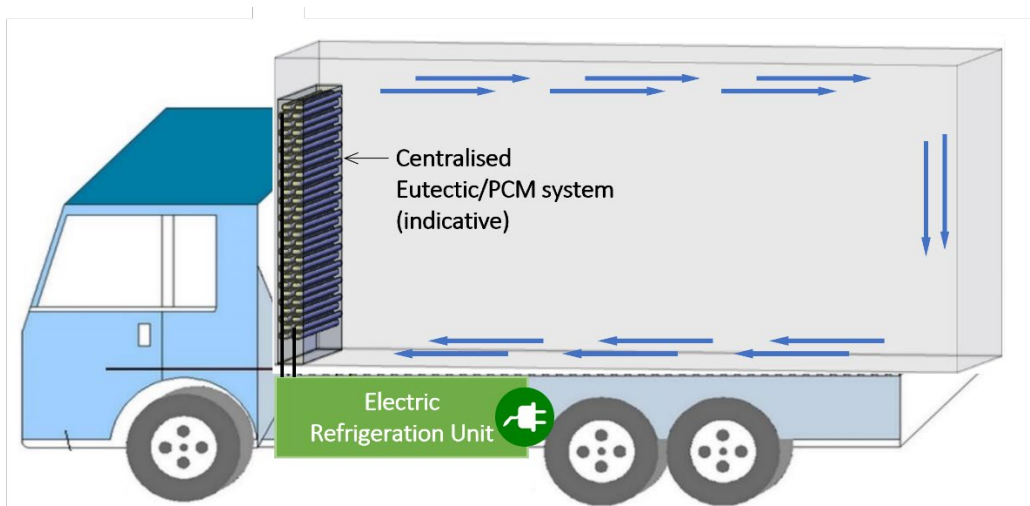
Figure 24. A schematic drawing of the novel eutectic refrigeration system (note: eutectic system is indicative only).

Five potential configurations were proposed and only two of them are illustrated in the drawings in Table 14 for confidentiality reasons. In the first configurations, the PCM is encapsulated in rectangular containers. The coolant tubes are embedded inside the PCM container, in which the refrigerant flows and freezes the PCM during charging. A fan is installed on the top of the PCM case to draw warm air from the bottom of the compartment. Passing through the void space between PCM containers, the warm air is cooled down and released from the top of the compartment. Configuration #2 is a typical shell-and-tube heat exchanger, in which the PCM is kept in the shell space and a secondary heat transfer fluid flows inside the tubes to transfer energy in/out of the PCM. Specifications are also given for indication purposes only and further optimisation of the design will be conducted when a specific design is selected. The advantages and disadvantages of the proposed configurations are discussed in Table 15.

Table 14. Design options and specifications for a novel eutectic refrigeration system.
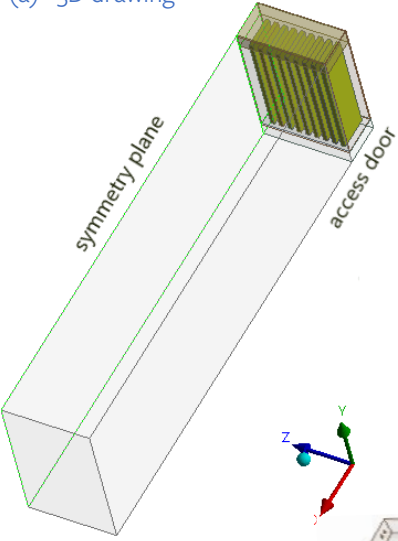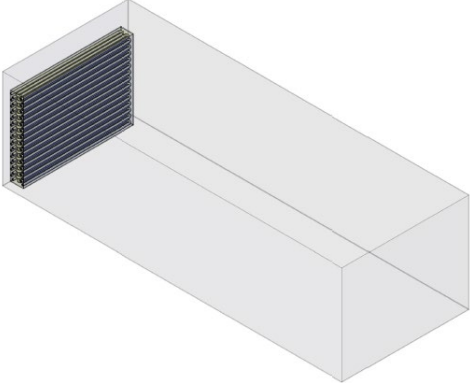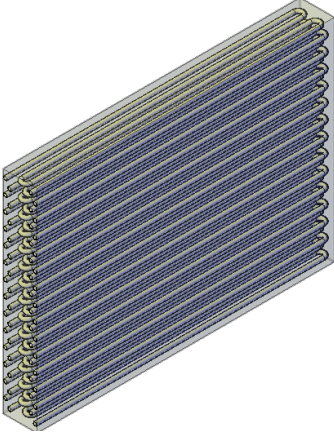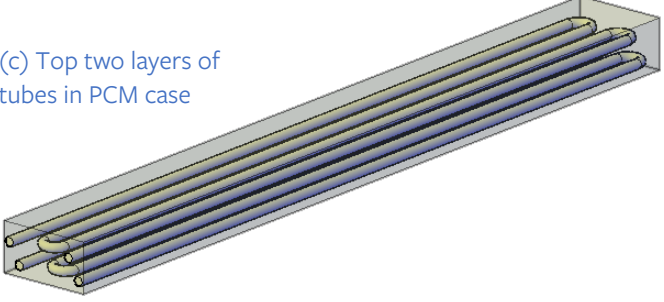
Configuration 1 - vertical medium-sized plates	Specifications
(a) 3D drawing (b) sectional view along z-axis (c) PCM plate with coolant tube	Number of plates: 18 Dimension of plate (length x width x thickness): 1.2 5m x 0.35 m x 0.045 m Heat transfer area: 15.75 m² Quantity of PCM: 457 kg Dimension of case (length x width x height): 1.75 m x 0.425 m x 1.25 m
Configuration 2 - shell-and-tube, PCM contained in the case	Specifications
(a) Refrigerated space (b) PCM case (c) Top two layers of tubes in PCM case	Number of heat transfer fluid (HTF) tubes: 28 Dimension of each HTF tube: 6.8 m (length) Outer tube diameter: 0.018 m Inner tube diameter: 0.015 m Heat transfer area: 9.8 m² Quantity of PCM: 500 kg Dimension of box (length x width x height): 1.75 m x 0.2 m x 1.25 m

Table 15. Advantages and disadvantages of five novel eutectic refrigeration configurations.

	Advantages	Disadvantages
Configuration 1 (vertical medium-sized plates)	o Medium heat transfer area to PCM mass/ volume ratio. o Low number of vessels initially needing to be manufactured for prototypes.	o Intermediate impact of individual vessel failure in relation to both thermal performance and spillage volume. o Intermediate individual vessel mass and likely associated stresses on each vessel.
Configuration 2 (shell-and-tube, PCM contained in the case)	o Half volume of PCM case compared to the others. o Only one vessel needing to be manufactured for prototypes.	o Relatively high potential impact of vessel failure in relation to both thermal performance and spillage volume. o Intermediate stresses on the vessel. o Need a fan coil unit to supply cold air and a secondary HTF to charge the eutectic system.

5.2   Numerical modelling

5.2.1   Modelling of current commercial eutectic truck

Commercially available eutectic trucks (Truck) have PCM plates installed under the roof and on the front of the container as shown in Figure 4. To understand the current performance benchmark of eutectic trucks it is important to understand the internal air pattern, thermal performance, and temperature uniformity under different indoor/outdoor conditions. Modelling the current design can help identify possible enhancements or alternative designs.

The modelling was conducted for a medium size commercial container of L=5.4 m, W=2 m, H=1.57 m with an aspect ratio (AR) of L/H = 3.3. The literature has identified this size as offering the best thermal performance (Kayansayan et al., 2017). A symmetrical model was prepared as shown in Figure 25a. The number and size of PCM plates were selected to replicate the commercial system, two plates with dimensions of L=1.60 m, W=0.49 m, H=0.045 m, and five plates with dimensions of L=1.75 m, W=0.7 m, H=0.045 m. The PCM plate included in the model had a refrigeration tube immersed in PCM as shown in Figure 25b.

(a)   (b)
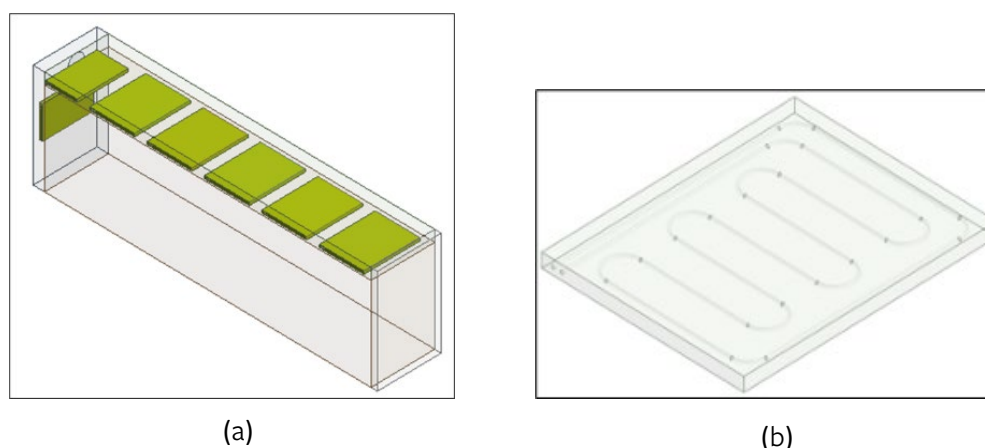
Figure 25. Model drawings, (a) a symmetrical model with the PCM plates at front and top, (b) a PCM plate with the refrigeration tube immersed in the PCM.

The impact on air and temperature profiles inside the refrigerated container can be examined using different outlet pressures and fan velocity. If a fan is excluded, due to its electricity consumption and

maintenance requirement, the natural convection prevails which may not be optimal for containers longer than four metres. The performance of natural convection diminishes with higher aspect ratio (L/H), and without a fan and forced convection, hot spots are more likely to form across a container.

CFD modelling assists with determining an optimum outlet pressure for each specific configuration. Figure 26 shows the air velocity when the outlet pressure from a fan at the front of the container is set to 50 Pa. The higher the pressure outlet from the fan, the higher the air velocity and circulation around the container. Higher air velocity results in a more intense air curtain at the back which is desired to reduce air infiltration particularly when doors are open. This can be seen in Figure 26a where the vector density covers the back door.

Air circulation can also impact the temperature distribution inside the refrigerated container (Figure 27a) and heat transfer from the walls of the container and PCM surfaces (Figure 27b). Figure 27b shows a higher heat transfer rate from the PCM plates closer to the fan which can reduce the temperature uniformity in the container. These results are from the preliminary study which shows the capability of the CFD study to examine the impact of different parameters on the flow, and thermal performance of the PCM system. In the next stage of this study, more modelling will be conducted to identify the impact of different parameters to assist in optimisation and detailed design.

Figure 26. Air velocity in the refrigerated container with 50 Pa fan outlet pressure, (a) axial velocity vectors, (b) axial velocity contours.

Figure 27. (a) Temperature distribution in the container, (b) Heat flux from the outer walls of the container and the PCM surfaces.
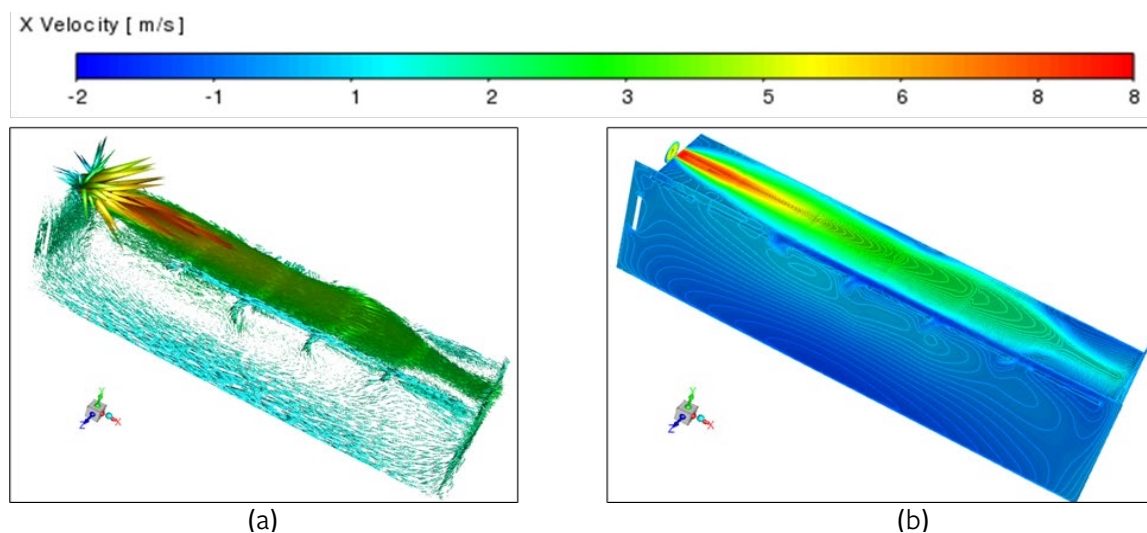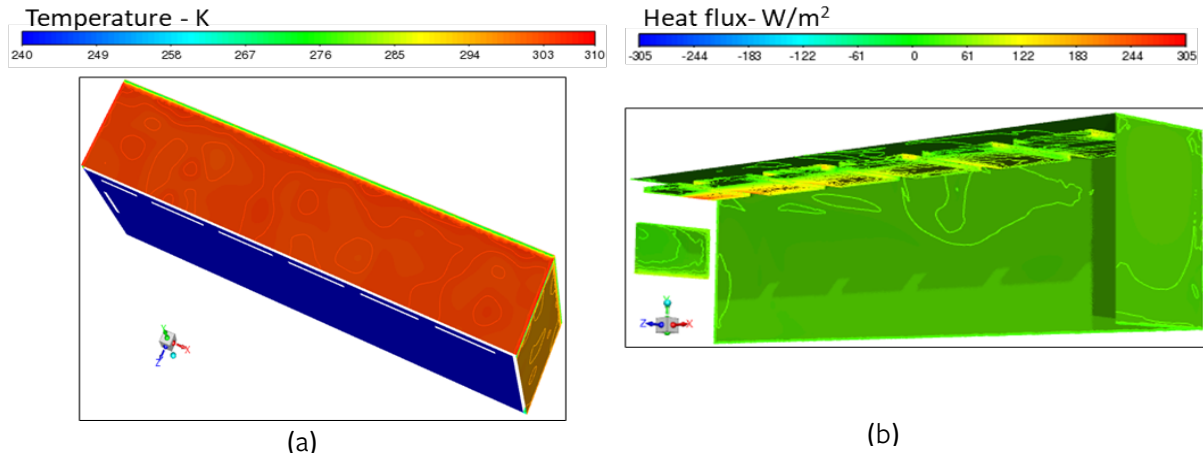
5.2.2   Modelling of the alternative proposed design

From the concept designs introduced in section 5.1, one centralised configuration was selected and modelled. This configuration has shown higher heat transfer area and the lowest individual size and mass of vessel.

A small size container with dimensions of L=4.2 m, W=2.2 m, H=1.9 m has been selected for the first size to be built by the industry partner, Aldom, for modelling the proposed configuration. Polyurethane was considered as insulation with thicknesses of 0.075 m for the top and 0.045 m for the back and side of the container. The insulation type and thicknesses were selected according to the recommendation by ASHRAE Refrigeration Handbook. Using polyurethane with thermal conductivity of 0.022 W/(m·K) results in less heat loss.

The results of preliminary transient modelling are shown in Figure 28 and Figure 29. Transient modelling is necessary to accommodate the melting of PCM.

Figure 28a shows the axial velocity vector with higher velocity at the fan outlet which reduces towards the back of the container. This velocity pattern is the result of fan outlet pressure equal to 50 Pa (relevant for small container with L=4 m considering the results of a previous study) which resulted in maximum velocity of 5 m/s. A higher velocity may be required for more air coverage at the back of container to prevent a high rate of air infiltration through the back doors. If so, a fan with outlet pressure higher than 50 Pa would be required.

Figure 28b shows the axial velocity contours and gradients further from the fan at the top and return to the PCM cassette entrance at the bottom. The air velocity is higher at the top and lower at the bottom of the container due to the fan location, however, the indoor velocity distribution is more uniform elsewhere. This model can provide more insights with the inclusion of the packages and pallets in the container, which will assist in the selection of all parameters to achieve a more uniform air velocity around the packages to keep the temperature low enough and preserve the product quality.
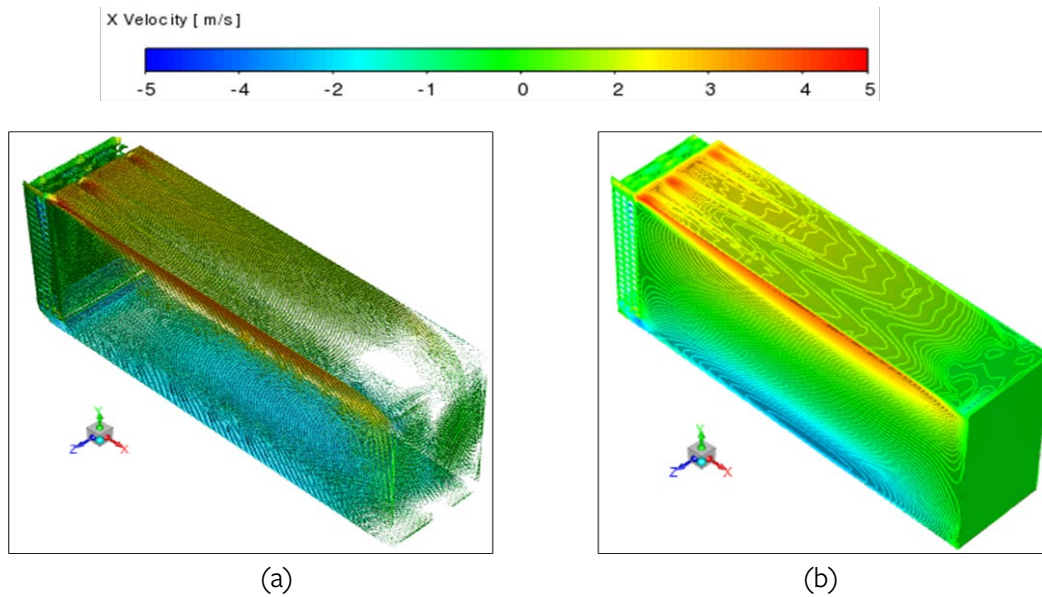
Figure 28. Air velocity in the refrigerated container with the proposed design and fan outlet pressure at 50 Pa, (a) axial velocity vectors, (b) axial velocity contours.
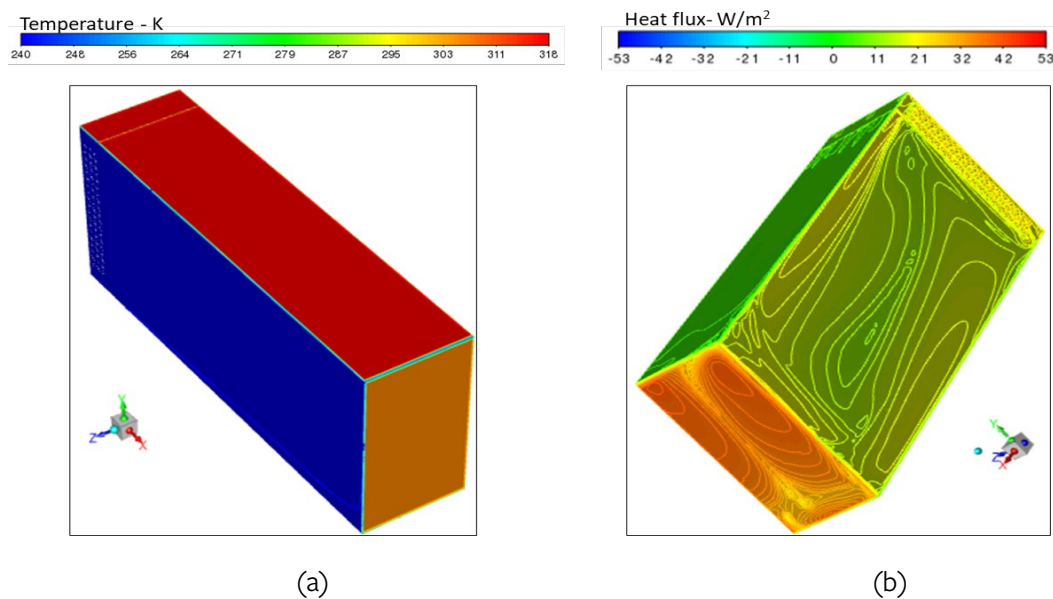
Figure 29. (a)Temperature distribution in (at symmetry) and outer surfaces of the container, (b) Heat flux from the outer walls of the container.

Figure 29a shows the temperature contours on the outer surfaces at the top, back and symmetry surface in the middle of the container. All the results are from the early stages of transient modelling after about 100 seconds which shows a low and uniform indoor temperature. Figure 29b shows the heat flux from the outer surfaces which is low at the top and side while it is higher at the back considering the cooling load due to air infiltration from the outside. Modelling of phase change processes is computationally demanding and requires a long time. In the next stage of the project, more insight will be acquired by modelling the proposed system during the melting process of the PCM.

5.3   Conclusion

Conventional refrigerated containers with PCM plates and a few alternative designs with PCM in a cassette were compared in this study. The distributed PCM plate system (commercially available) and the alternative PCM centralised system has the potential to be an optimum system for a specific application. Therefore, a detailed study including modelling and a parametric analysis is required to propose a suitable PCM system for each application.

Preliminary modelling of the commercially available and the proposed centralised system was conducted to show the capability of modelling to replicate indoor conditions inside a refrigerated container with different PCM systems. The preliminary design and modelling provided some insights into conventional refrigerated containers with PCM plates and the alternative design. The results indicate the following:

Air circulation impacts the temperature distribution inside the refrigerated container and the heat transfer from the walls of the container and PCM surfaces.

A higher fan outlet pressure results in higher outlet air velocity and an intense air curtain at the back which is desired to reduce air infiltration particularly when doors open.

The heat transfer from the PCM plate closer to a fan outlet can be higher than the PCM plates closer to the back of the container.

Modelling the selected centralised configuration showed a uniform air velocity distribution except close to the top and bottom of the container due to the fan location at the top.

However, a parametric study is required for the optimisation of the PCM system in the next stage of the project. The optimisation study will identify a design where a uniform air circulation and temperature provides minimum heat loss to the outside and a more uniform temperature inside preserving the food quality during transport.

6. Scheduling of Charging

6.1   Charging rate and duration

How and where a refrigeration system is 'recharged', and the charging duration, will depend on the type of refrigeration system.

There are three ways to recharge a battery-powered VCR system:

- o **Battery swapping** at a depot enables fast turnaround, and the charging of batteries can be scheduled to manage the cost and power demand of recharging, but it requires special equipment for swapping batteries, standardised batteries, and more batteries than trucks.
- o **AC charging** typically uses an on-board charger that converts a standard AC supply to the DC power required to recharge the battery. The charging rate for EV chargers is usually 7 kW for a single-phase connection up to 22 kW for a 3-phase connection, so it can take several hours to recharge a battery. AC supply equipment is inexpensive and can be installed at depots and at destinations.
- o **DC charging** uses an off-board charger to covert an AC supply to DC and can transfer power at higher rates than typical on-board chargers—up to 350 kW. A lithium-ion battery can typically be charged to around 80% full in 20–30 minutes, and thereafter the charging rate must be reduced as the battery becomes full. Charging rate limits will vary with the capacity of the charger, the capacity of the battery, the battery chemistry and the charging profiles implemented in the battery management system. If fast, full charging is critical then these need to be taken into account in the charge scheduling. However, DC charging equipment is expensive and requires a high-power connection to the electricity supply.

A **eutectic system with on-board refrigeration** can be recharged by plugging into the grid at a depot or at a destination. Eutectic trucks on the market typically charge at 3 kW (electrical), which is slower than charging a battery. However, the eutectic system can be given a partial recharge whenever the truck is stopped and power is available.

A **eutectic system with off-board refrigeration** can be recharged by pumping a coolant through the eutectic system at the depot. The charging rate depends on the design of the eutectic system and the temperature of the coolant. Cold coolant can be prepared and stored while the truck is on the road, allowing for "smart scheduling" to manage cost and power demand. There are not currently any off-board eutectic refrigeration systems commercially available.

A **eutectic swap** system is like a battery swap system. Spare eutectic packs can be cooled at the depot while the truck is on the road, then swapped into the truck using special handling equipment. Recharging of the eutectic packs can be scheduled to manage cost and power demand.

6.2   Cost

The cost of energy for recharging will depend on the electricity tariff:

- Some users are on a **single rate tariff** or a **block tariff**, where the cost per kilowatt-hour of electricity depends on the total consumption within a billing period but does not vary with the time of day. These tariffs are often associated with older electricity meters that measure how much electricity was used in a billing period but not when it was used. These tariffs are generally being replaced as newer 'interval' meters are rolled out.
- A **time-of-use** tariff varies the price of electricity with the time of day. Price is low at times when demand on the grid is usually low, typically overnight, and high at times when demand on

the grid is usually high. In South Australia, which has a high proportion of renewables, network prices are lowest in the "solar sponge" period between 10:00 and 15:00, when solar generation is usually high and demand is usually low. Prices can also vary with season.

- A **real-time** tariff or **pass-through** tariff is typically a combination of wholesale energy prices, which change every five minutes, and time-of-use or flat network tariffs. The wholesale price of electricity can vary from –$1,000/MWh when demand is low and there is a large amount of renewable energy generation available, up to $15,500/MWh when demand is high and generation is restricted.
- Some users, particularly business users, may be subjected to **demand charges** that depend on the maximum power use in a month or year.
- Some users may be subjected to **critical peak pricing**, where they are given lower prices most of the time but high prices during critical peak demand events that are announced in advance.
- **Demand management incentives** from network operators may be available to some users, who can be paid to reduce their demand during periods of high demand on the grid. The demand response standard AS4755 also allows remote agents, such as network operators, to request increases in demand.

Single rate tariffs and **block tariffs** do not offer any cost incentives for managing when recharging occurs.

Time-of-use prices are predictable, so it is straightforward to design a charging schedule that minimises the cost of recharging. Systems with storage (battery swap, off-board eutectic charging with storage and swappable eutectic packs) allow greater scheduling flexibility than systems that require the truck to be present when recharging.

Real-time prices change every five minutes and can be difficult to predict. The Australian Energy Marker Operator (AEMO) publishes predictions of 30-minute prices up to 48 hours in advance; these can be used to help plan charging schedules.

Critical peak pricing and **demand management incentives** can be handled in the same way as wholesale price predictions.

Managing **demand charges** requires coordination of cooling system recharging with other loads on site—you need to predict when the recharging depot's highest demand for the month (or year) will occur and minimise charging at that time.

For a business where the truck schedules are predetermined and allow sufficient time for charging, designing a charging strategy that minimises cost or maximises the use of renewable energy is a straightforward optimisation problem, but the formulation and solution of the scheduling problem must be tailored to each business, as it depends on:

- the electricity tariff (if you want to minimise cost)
- when renewable energy is available (if you want to maximise the use of renewable energy)
- when the trucks, batteries or eutectic systems are available for charging
- charging characteristics of the trucks, batteries or eutectic systems
- constraints on the number of charging stations available
- constraints on the amount of site power that can be used for charging at any time.

The problem is more challenging for businesses where the truck schedules can be varied to allow cheaper or cleaner charging, since this requires simultaneous scheduling of deliveries and charging.

In the next phase of the project, a charging schedule will be developed to manage the electricity demand and minimise the cost for a single vehicle and a fleet of vehicles, depending on the charging rate, charging duration and electricity tariff.

7. Conclusions

Firstly, this report has covered the literature review on transport refrigeration systems including the state-of-the-art technologies and emerging technologies enabling better performance in terms of reducing energy cost, reducing CO_2-e gas emissions, improving energy efficiency of the refrigeration system, and improving temperature management. PCM candidates, having the potential to be used for both frozen and fresh produce delivery, were identified from the literature and characterised to measure their thermophysical properties, such as the melting temperature, latent heat of fusion, specific heat capacity, density and thermal conductivity. Four candidates with high energy density were selected for further investigation and evaluation.

Secondly, the CO_2-e emissions (to refrigerate the produce), weight and cost of the diesel-powered refrigeration, battery-powered refrigeration and eutectic refrigeration system were studied and compared. Using the existing diesel-powered refrigeration system as a baseline, eutectic refrigeration was found to reduce CO_2-e gas emissions by 70%. However, it slightly increases the weight of the vehicle by 167 kg if the refrigeration unit is on-board. Battery-powered refrigeration, as a strong competitor, weighs less than the eutectic system if the specific energy of the battery is greater than 150 Wh/kg, which can be easily achieved with modern batteries. However, even with falling battery prices, battery-powered systems are still expected to be more expensive than eutectic refrigeration up to 2030. Furthermore, eutectic refrigeration systems have the lowest operating cost when an off-peak tariff is assumed for charging at $0.275/kWh. Depending on the charging rate, charging duration and electricity tariff, charging could be scheduled to manage the demand and minimise the cost. This will be further investigated in the next phase of the project.

Five different concept designs were proposed. For confidentiality reasons, two of them are presented in this report with their advantages and disadvantages discussed. The centralised design has the advantages of easy maintenance and better temperature control. After consultation with industry and considering the pros and cons of all the concept designs, one configuration was selected due to the advantages of high ratio of heat transfer area to PCM mass/volume, low individual vessel mass and likely associated stresses on each vessel and relatively low potential impact of individual vessel failure in relation to both thermal performance and spillage volume.

Finally, the preliminary modelling results of the current and proposed configurations are presented in this report to design an optimum PCM system for a prototype. An optimum PCM system will achieve uniform air and temperature distribution and low heat loss. The first CFD analysis analysed an existing commercial eutectic truck which provided some insight into the flow and thermal performance of the system. A novel eutectic refrigeration system was then analysed and the results showed that this system was promising for delivering a high flow and thermal performance. Moreover, this configuration is highly adaptable to specific design criteria for stationary and mobile applications with various sizes, temperature requirements and climate conditions.

For the next phase of the project, a prototype of the selected system will be constructed and demonstrated on a refrigerated body to verify the concept. The thermal performance of the prototype will be evaluated by monitoring internal temperatures in various ambient conditions.

Reference

A2EP. (2017a). *Food cold chain optimisation: Improving energy productivity using real time food condition monitoring through the chain.* https://www.a2ep.org.au/publications

A2EP. (2017b). *Innovation to improve energy productivity in the food value chain.* https://www.a2ep.org.au/publications

A2EP. (2017c). *A roadmap to double energy productivity in freight transport by 2030.* https://www.a2ep.org.au/publications

Adekomaya, O., Jamiru, T., Sadiku, R., & Huan, Z. (2016). Sustaining the shelf life of fresh food in cold chain – A burden on the environment. *Alexandria Engineering Journal, 55*(2), 1359-1365. https://doi.org/https://doi.org/10.1016/j.aej.2016.03.024

Advanced Transport Refrigeration & AirConditioning. (2021). *New Innovative Technology that will Transform the Refrigerated Transport Industry.* https://www.atrplus.com.au/cool-news-room/mitsubishi-te30-reefer-unit

Air Resources Board. (2015). *Technology Assessment: Transport Refrigerators.* https://ww2.arb.ca.gov/sites/default/files/2020-06/TRU%20Tech%20Assessment%20Report%20ada.pdf

ASHRAE. (2018). Chapter 24: Refrigerated-facility loads. In *ASHRAE Handbook of Refrigeration.* American Society of Heating, Refrigerating and Air Conditioning Engineers, Inc.

Australian Food and Grocery Council. (2017). *Australian Cold Chain Guidelines 2017.* https://www.afgc.org.au/wp-content/uploads/2019/07/Australian-Cold-Chain-Guidelines-2017.pdf

Australian Trucking Association. (2021). Safer Freight Vehicles Discussion Paper. https://www.truck.net.au/sites/default/files/submissions/20210630ATAsubmissionSaferFreightVehicles.pdf

Ben Taher, M. A., Kousksou, T., Zeraouli, Y., Ahachad, M., & Mahdaoui, M. (2021). Thermal performance investigation of door opening and closing processes in a refrigerated truck equipped with different phase change materials. *Journal of Energy Storage, 42*, 103097. https://doi.org/https://doi.org/10.1016/j.est.2021.103097

Brodribb, P., & McCann, M. (2020). *A study of waste in the cold food chain and opportunities for improvement* https://www.environment.gov.au/protection/ozone/publications/waste-study-cold-food-chain-improvement-opportunities

Brodribb, P., McCann, M., & Dewerson, G. (2021). *Cold Hard Facts 2021.* https://www.agriculture.gov.au/sites/default/files/documents/cold-hard-facts-2021.pdf

Carrier Transicold. (2018). Free your refrigeration from emissions. In C. Transicold (Ed.).

Carrier Transicold. (2021a). *Carrier Transicold Enters Strategic Agreement with AddVolt* https://www.carrier.com/truck-trailer/en/eu/news/news-article/carrier-transicold-enters-strategic-agreement-with-addvolt.html

Carrier Transicold. (2021b). *FresH2 Hydrogen Fuel Cell Refrigerated Transport Project Enters Road Testing Phase* https://www.carrier.com/truck-trailer/en/eu/news/news-article/fresh2-hydrogen-fuel-cell-refrigerated-transport-project--enters-road-testing-phase.html

Carrier Transicold. (2021c). FresH2 refrigerated transport project starts road testing in France. *Fuel Cells Bulletin, 2021*(10), 4-5. https://doi.org/https://doi.org/10.1016/S1464-2859(21)00544-7

Clean Energy Regulator. (2022). *EERS release 2021–22.* https://www.cleanenergyregulator.gov.au/OSR/EERS/eers-current-release

Colbourne, D., Solomon, P., Wilson, R., De Swardt, L., Schuster, M., Oppelt, D., & Gloël, J. (2016). Development of R290 transport refrigeration system. Refrigeration Science and Technology,

Department of Agriculture. (2014). *Australian Food Statistics 2012-13.* https://www.agriculture.gov.au/sites/default/files/sitecollectiondocuments/ag-food/publications/food-stats/australian-food-statistics-2012-13.pdf

Department of Climate Change, Energy, the Environment and Water (2022). *Australian National Greenhouse Accounts Factors: 2022.* Australian Government. Retrieved 19 December from

https://www.dcceew.gov.au/climate-change/publications/national-greenhouse-accounts-factors-2022

Estrada-Flores, S., & Tanner, D. (2008). RFID Technologies for Cold Chain Applications. *Review article, Intergovernmental Organization for the Development of Refrigeration, Bulletin, 4,* 4-9.

Food Logistics. (2008). Thinking Out Of The Box. https://www.foodlogistics.com/transportation/cold-chain/article/10315594/thinking-out-of-the-box

Gaton, B. (2021). How much does it cost to replace the batteries in electric vehicles? *The Driven.* https://thedriven.io/2021/07/23/how-much-are-replacement-batteries-for-electric-vehicles-in-australia/

Han, A. (2005). Transporting refrigerated food. *Food Technology.* https://www.foodprocessing.com.au/content/materials-handling-storage-and-supply-chain/article/transporting-refrigerated-food-957739851

Han, B., Choi, J. H., Dantzig, J. A., & Bischof, J. C. (2006). A quantitative analysis on latent heat of an aqueous binary mixture. *Cryobiology, 52*(1), 146-151.

Kayansayan, N., Alptekin, E., & Ezan, M. A. (2017). Thermal analysis of airflow inside a refrigerated container. *International Journal of Refrigeration, 84,* 76-91. https://doi.org/https://doi.org/10.1016/j.ijrefrig.2017.08.008

König, A., Nicoletti, L., Schröder, D., Wolff, S., Waclaw, A., & Lienkamp, M. (2021). An Overview of Parameter and Cost for Battery Electric Vehicles. *World Electric Vehicle Journal, 12*(1), 21. https://www.mdpi.com/2032-6653/12/1/21

Kujak, S., & Schultz, K. (2018, 6-8 April 2018). Low GWP refrigerant options and their LCCP impact for transport refrigeration products. 5th IIR International Conference on Sustainability and the Cold Chain., Beijing, China.

Lafaye de Micheaux, T., Ducoulombier, M., Moureh, J., Sartre, V., & Bonjour, J. (2015). Experimental and numerical investigation of the infiltration heat load during the opening of a refrigerated truck body. *International Journal of Refrigeration, 54,* 170-189. https://doi.org/https://doi.org/10.1016/j.ijrefrig.2015.02.009

Li, Y., Li, C., Lin, N., Xie, B., Zhang, D., & Chen, J. (2021). Review on tailored phase change behavior of hydrated salt as phase change materials for energy storage. *Materials Today Energy, 22,* 100866.

Liu, M., Saman, W., & Bruno, F. (2012). Development of a novel refrigeration system for refrigerated trucks incorporating phase change material. *Applied Energy, 92*(0), 336-342. https://doi.org/10.1016/j.apenergy.2011.10.015

Liu, W., Placke, T., & Chau, K. T. (2022). Overview of batteries and battery management for electric vehicles. *Energy Reports, 8,* 4058-4084. https://doi.org/https://doi.org/10.1016/j.egyr.2022.03.016

Lu, W., Liu, G., Xing, X., & Wang, H. (2019). Investigation on Ternary Salt-Water Solutions as Phase Change Materials for Cold Storage. *Energy Procedia, 158,* 5020-5025. https://doi.org/https://doi.org/10.1016/j.egypro.2019.01.662

Maiorino, A., Petruzziello, F., & Aprea, C. (2021). Refrigerated Transport: State of the Art, Technical Issues, Innovations and Challenges for Sustainability. *Energies, 14*(21), 7237. https://doi.org/10.3390/en14217237

Mark Ellis & Associates Pty Ltd. (2009). *In from the cold: Strategies to increase the energy efficiency of non-domestic refrigeration in Australia and New Zealand for Federal Dept of Climate Change & Energy Efficiency.* https://www.energyrating.gov.au/sites/default/files/documents/200912b-in-from-the-cold-technical-vol2%5B1%5D.pdf

Oró, E., De Gracia, A., Castell, A., Farid, M. M., & Cabeza, L. F. (2012). Review on phase change materials (PCMs) for cold thermal energy storage applications. *Applied Energy, 99,* 513-533.

Rai, A., & Tassou, S. A. (2017). Environmental impacts of vapour compression and cryogenic transport refrigeration technologies for temperature controlled food distribution. *Energy Conversion and Management, 150,* 914-923. https://doi.org/https://doi.org/10.1016/j.enconman.2017.05.024

Ramaube, M., & Huan, Z. (2019). Testing and Performance Evaluation of a R404A Transport Refrigeration System Retrofitted With R290. The 17th Industrial and Commercial Use of Energy (ICUE) Conference 2019, Cape Town, South Africa.

Resalati, S., Okoroafor, T., Henshall, P., Simões, N., Gonçalves, M., & Alam, M. (2021). Comparative life cycle assessment of different vacuum insulation panel core materials using a cradle to gate approach. *Building and Environment, 188*, 107501. https://doi.org/https://doi.org/10.1016/j.buildenv.2020.107501

Senguttuvan, S., Rhee, Y., Lee, J., Kim, J., & Kim, S.-M. (2021). Enhanced heat transfer in a refrigerated container using an airflow optimized refrigeration unit. *International Journal of Refrigeration, 131*, 723-736. https://doi.org/https://doi.org/10.1016/j.ijrefrig.2021.02.017

Senguttuvan, S., Youn, J.-S., Park, J., Lee, J., & Kim, S.-M. (2020). Enhanced airflow in a refrigerated container by improving the refrigeration unit design. *International Journal of Refrigeration, 120*, 460-473. https://doi.org/https://doi.org/10.1016/j.ijrefrig.2020.08.019

SOLGroup. (2022). *HFC Refrigerant Gases*. Retrieved April 4 from https://www.sol.it/en/products-and-services/our-products-and-services-for-industry/refrigerant-gases-and-natural-fluid-refrigerants/hfc-refrigerant-fluid#:~:text=Freons%20or%20hydrofluorocarbons%20(HFC)%20are,which%20damage%20the%20ozone%20layer.

Swahn, M. (2008). *Draft report: Additional CO2e factors in goods transport*. https://www.transportmeasures.org/wp-content/uploads/2015/11/Additional-energy-use-in-transport-sector-20080611-rev-20102411.pdf

Tassou, S. A., De-Lille, G., & Ge, Y. T. (2009). Food transport refrigeration – Approaches to reduce energy consumption and environmental impacts of road transport. *Applied Thermal Engineering, 29*(8), 1467-1477. https://doi.org/10.1016/j.applthermaleng.2008.06.027

Tassou, S. A., Hadawey, A., Ge, Y., & Groutte, B. L. d. (2009). Carbon Dioxide Cryogenic Transport refrigeration Systems.

Truck, F.   https://www.framectruck.com/eng/

Wu, T., Xie, N., Niu, J., Luo, J., Gao, X., & Zhang, Z. (2020). Preparation of a low-temperature nanofluid phase change material: MgCl2–H2O eutectic salt solution system with multi-walled carbon nanotubes (MWCNTs). *International Journal of Refrigeration, 113*, 136-144.

Xie, N., Li, Z., Gao, X., Fang, Y., & Zhang, Z. (2020). Preparation and performance of modified expanded graphite/eutectic salt composite phase change cold storage material. *International Journal of Refrigeration, 110*, 178-186.

Xing, X., Lu, W., Zhang, G., Wu, Y., Du, Y., Xiong, Z., Wang, L., Du, K., & Wang, H. (2022). Ternary composite phase change materials (PCMs) towards low phase separation and supercooling: eutectic behaviors and application. *Energy Reports, 8*, 2646-2655. https://doi.org/https://doi.org/10.1016/j.egyr.2021.12.069

Yang, L., Villalobos, U., Akhmetov, B., Gil, A., Khor, J. O., Palacios, A., Li, Y., Ding, Y., Cabeza, L. F., & Tan, W. L. (2021). A comprehensive review on sub-zero temperature cold thermal energy storage materials, technologies, and applications: State of the art and recent developments. *Applied Energy, 288*, 116555.

Zhang, X., Shi, Q., Luo, L., Fan, Y., Wang, Q., & Jia, G. (2021). Research Progress on the Phase Change Materials for Cold Thermal Energy Storage. *Energies, 14*(24), 8233.

Appendix: Summary of Knowledge Sharing Activities

The focus of sharing of knowledge in this project is related to electrification of cold chain, thermal energy storage technology and management of electricity grid stability. To ensure stakeholders were informed and engaged, the following activities were carried out.

- Participation and presentation in the RACE for 2030 CRC SA Meeting on the 23rd of June 2022 and the meeting with Aldom Transport Engineering and Aldom's industry partners.
- Research outcomes and findings will be shared to public through RACE for 2030 and UniSA websites and a webinar.
- A webpage has been developed by RACE for 2030 CRC.